Basic Radiation Physics

1

Taher Hosny, Eman Al-Anezi, and Magdy M. Khalil

Contents

T. Hosny
Nuclear Medicine and Cyclotron Department,
King Hamad University Hospital, Busaiteen, Bahrain

Biophysics Department, Faculty of Science,
Cairo University, Giza, Egypt
e-mail: Taher_Hosny@outlook.com

E. Al-Anezi
Nuclear Medicine and Cyclotron Department,
King Hamad University Hospital, Busaiteen, Bahrain
e-mail: Eman-al-anzy@hotmail.com

M.M. Khalil, PhD (✉)
Medical Biophysics, Department of Physics, Faculty of Science, Helwan University, Cairo, Egypt
e-mail: Magdy_khalil@hotmail.com

Abstract

This chapter provides a comprehensive overview of essential radiation physics required to understand many fundamental concepts of nuclear medicine in general and positron emission tomography (PET) imaging in particular. We aimed to introduce the most important elements of radiation physics as tightly related to daily practice and routine activities performed in clinical environment. Topics covered in this chapter have discussed definition of electromagnetic radiation, atomic models, atomic structure, radio-

M.M. Khalil (ed.), *Basic Science of PET Imaging*, DOI 10.1007/978-3-319-40070-9_1

activity and radioactive modes of decay; production of radiopharmaceuticals including medical cyclotrons, saturation yield and reactor-produced radionuclides; and interaction of radiation with matter, linear and mass attenuation coefficients as well as mostly commonly used radiation detection and measurement devices. As this is the first chapter in the book, we made every effort to cover as many aspects that might come across the reader throughout or facilitate the understanding of other chapters.

1.1 Introduction

Radiation physics does broaden our understanding of many facts and theories that underlie clinical application of radioisotopes in medicine and other areas of biomedical research. More specifically, nuclear medicine practitioners are among those that must always keep an eye not only on fundamental radiation and nuclear physics but also on how this can be utilized and applied in practice. Many of the achievements in nuclear medicine were in large part related to those concepts with particular benefits to diagnostic imaging and radionuclide therapy. Therefore, it is an important course for those who attempt to learn the underlying bases such as the structure of the atom, electron as well as nuclear binding energy, radioactivity and its associated formulae, units and conversions in addition to production of radiopharmaceuticals, interaction of radiation with matter and other safety and radiation protection devices and measurements. Electromagnetic radiation and its associated wide spectrum, duality principle, structure of the atom, atomic models proposed over the years, mass defect and nuclear binding energy and other important issues are among the first topics that we will start with.

1.2 Electromagnetic Radiation

Electromagnetic radiation (EM) consists of self-sustaining oscillating electric and magnetic fields at right angles but in phase and perpendicular to each other and to the direction of propagation as shown in Fig. 1.1. It does not require a supporting medium and travels through empty space at the speed of light. EM radiation exhibits wave properties as well as particulate properties (duality principle). All different kinds of electromagnetic radiation (microwaves, radio waves, infrared, x-ray, gamma ray, etc.) differ in one important property which is its specific wavelength. When electromagnetic radiation is spread out according to its wavelength, the result is electromagnetic spectrum as explained in Fig. 1.2. The electromagnetic spectrum is divided into five major types of radiation. These include radio waves (including microwaves), light (including ultraviolet, visible and infrared), heat radiation and ionizing radiation such as x-rays and gamma rays.

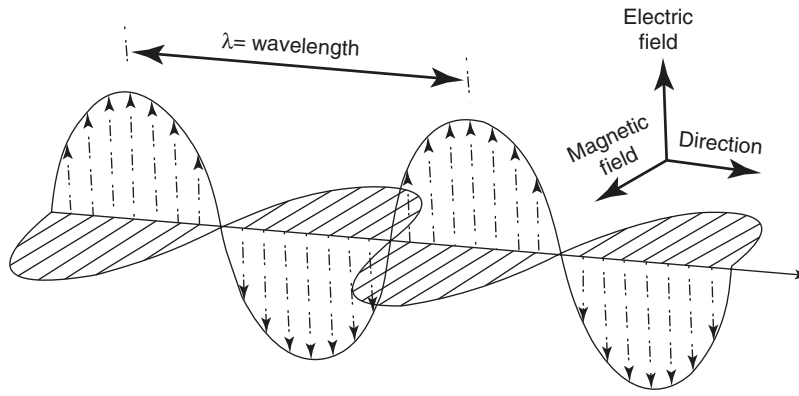

Fig. 1.1 Electric and magnetic field propagated as a transverse wave perpendicular to each other and perpendicular to the direction of propagation

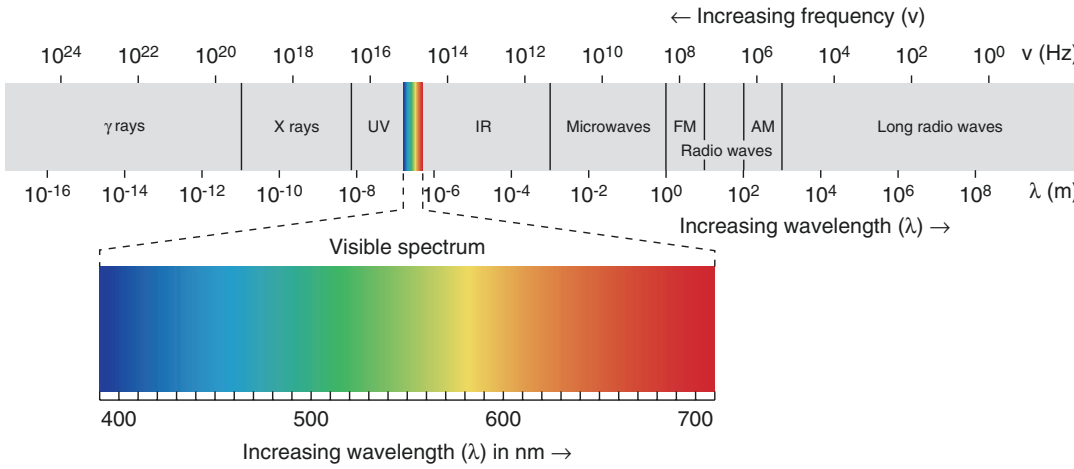

Fig. 1.2 Electromagnetic spectrum: Waves with shorter wavelength will have high frequency and vice versa. Ionizing radiation with high frequency is more energetic and can induce biological effects

1.2.1 Wave/Particulate Nature of Radiation

Although wave and particle having different physical characteristics, electromagnetic radiation can behave as both at once (wave-like and particle-like). Many experiments showed that radiation is sometimes behaves as wave and sometimes behaves as particle concluding that wave and particle cannot be separated, only together the phenomena can be explained. This has been proposed by a number of scientists leading to the theory of wave – particle duality.

1.2.2 Duality Principle

The duality principle describes the elementary particles and electromagnetic radiation in terms of wave and particle-like characteristics. It was not originated from a single scientist or revealed from only one experiment. Max Plank has stated that energy is transferred in a form of packets or quanta, while Albert Einstein thought of light as particle-like or localized in packets of discrete energy in contrast to its original definition as wave-like properties. Another contribution came from the phenomenon of photoelectric effect proposed also by Einstein. He stated that the emission of photoelectrons from metal plates does occur if and only if the incident photons on photoemissive plate have a threshold wavelength of energy that is able to liberate electrons from the metal. Then, Louis de Broglie proposed that electrons and other particles can behave as waves and has wavelength and frequencies. While this proposal was in 1927, the announcement of the understanding of the wave and particle aspects of matter was carried out in 1928. See Fig. 1.3.

Radiation can be described in terms of packet of energy, called photons. The energy of a photon is given by

$$E\left(\text{photon}\right) = h\nu = hc/\lambda \qquad (1.1)$$

where h is plank's constant ($h = 6.625\ 6 \times 10^{-34}$ J s); ν and λ are characteristics frequency and wavelength, respectively; and c is the speed of light in vacuum (Table 1.2).

Waves are characterized by frequency, wavelength and phase. Electromagnetic radiation is massless with no charge, while wavelength and frequency of oscillating fields are related to each other by the following equation:

$$c = \lambda\nu \qquad (1.2)$$

However, they are still affected by gravity.

It is of relevance to mention here that many diagnostic imaging modalities rely heavily on physical properties of different electromagnetic radiations. For example, in x-ray computed tomography (CT), a uniform x-ray beam interacts with

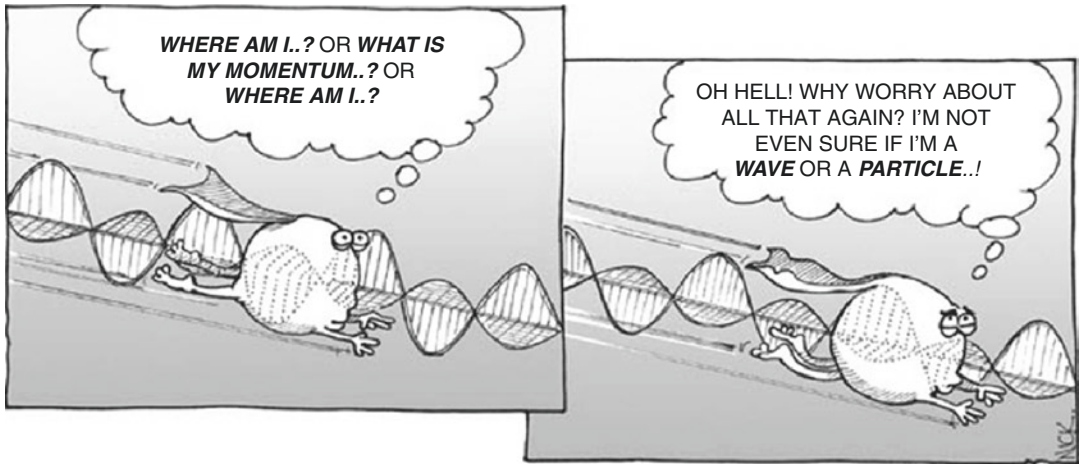

Fig. 1.3 Duality principle: Particles and electromagnetic radiation possess waves and particle characteristics (From http://www.lab-initio.com/quantum.html)

the human tissues, and the transmitted amount is measured by the CT detector to reveal an image that reflects the attenuation properties of the tissue covered in the scanning beam. Radiologic techniques such as fluoroscopy, angiography and x-ray radiography are also dependent on x-ray radiations in eliciting important diagnostic information for a wide range of human diseases and abnormalities.

Electromagnetic radiation is also associated with nuclear medicine in the sense that gamma emission is used in many diagnostic purposes utilizing the powerful penetrating capabilities of the radiation beam. This essentially takes place when patient is injected with pharmaceutical compound labelled to gamma-emitting radionuclide. After radiopharmaceutical administration, the body tissue will be the source of gamma ray emission that is used in the imaging process.

Another application of electromagnetic radiation in clinical practice is magnetic resonance (MR) imaging which is different from other imaging techniques such as CT and nuclear medicine, as it uses radio frequency (i.e. radio wave) as energy source rather than ionizing radiation. The procedure requires the usage of a strong magnetic field for spin alignment of hydrogen nuclei in the body. The spin synchronizes as the radio-frequency pulse matches the nuclear resonance frequency of the protons.

While radio wave energy is consistent with energy of nuclear spin in magnetic field, microwave matches rotational energy of the molecule. The infrared (IR) region in the spectrum lies beyond the region that the human eye perceives as red light. The absorption of infrared light causes increases in the frequencies at which the bonds between atoms stretch and bend. This is the idea behind infrared spectroscopy where there is a sort of matching between the IR radiation energy and the frequency of a specific molecular motion usually bond bending or stretching. However, the higher-frequency ultraviolet radiation that lies above the visible limit of the light spectrum is matching to different electronic transition states. In summary:

- Radio → nuclear spin in magnetic field
- Microwave → rotation
- Infrared → vibration
- Ultraviolet → electronic

1.3 Atomic Models

Atom is considered as the basic building unit of an element. An atom is the smallest unit of element that retains its physical and chemical properties. Each known element has atoms differ from the atoms of other elements; this gives each element a unique atomic structure. Many atomic models were proposed, and some have been adopted as ways to describe the atom. Neither of them is perfect, but they have relative contribu-

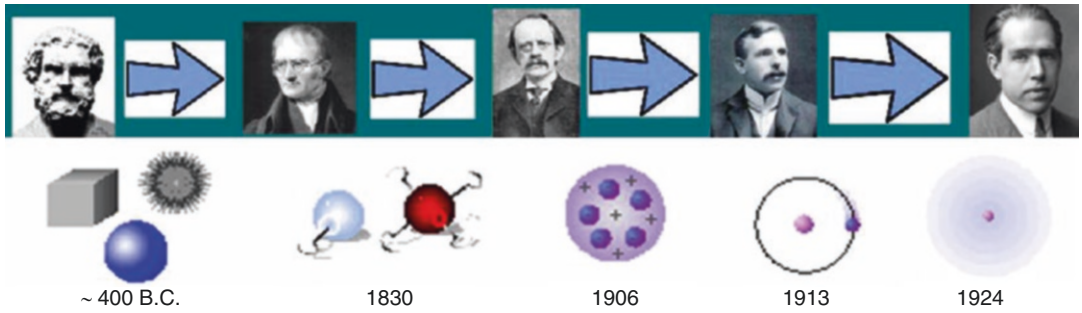

Fig. 1.4 Serial time line of atomic models proposed over the years and described by the following scientists (*left to right*): Democritus, Dalton, Thomson, Rutherford and Bohr. Taken from http://www.K12tlc.net/content/atomhist.htm

tions towards understanding these building blocks. See Figure 1.4 serial time line of atomic models.

1.3.1 History of Atomic Models

The first atomic model described in the literature is dated back to the Greek philosopher Democritus. He postulated the existence of invisible atoms, which are characterized only by quantitative properties such as size, shape and motion. His model described the atom as indivisible spheres representing the smallest piece of an element that still behave like the entire chunk of matter. There were no significant advances in definition and characterization of the atom until the English chemist John Dalton started to look at this in the 1800s. Dalton shared the same thoughts and impression as Democritus about atom in the sense that it is tiny and indivisible particles, but he introduced new assumptions about atom. The main assumptions of Dalton model were:

- All matter was composed of atoms, indivisible and indestructible. While all atoms of an element are identical and have the same properties, different elements have atoms of different size and mass.
- All compounds are composed of combinations of these atoms in defined ratios.
- Atoms can combine to form different compounds (e.g. carbon and oxygen combine to form carbon monoxide CO and carbon dioxide CO_2).
- Chemical reactions resulted in rearrangement of the reacting atoms.

In 1897, J.J. Thomson discovered the electron in series of experiments designed to study the nature of electric discharge in a high-vacuum cathode ray tube. In 1904, Thomson introduced a new atom model that differs from pervious atom models suggesting that the atom is uniform sphere of positively charged matter in which electrons are positioned by electrostatic forces.

A monumental breakthrough came in 1911 based on experimental results when Ernest Rutherford and his colleagues Hans Geiger and Ernest Marsden conducted the famous gold foil experiment intended to determine angles through which a beam of alpha particles (helium nuclei) would scatter after passing through a thin foil of gold. It was a new but exciting moment when they found few alpha particles recoiled almost directly backwards. It was Rutherford's interpretation that this happen when a positively charged and relatively heavy target particle, such as the proposed nucleus, could account for such strong repulsion. The negative electrons that balanced electrically the positive nuclear charge were regarded as travelling in circular orbits around the nucleus (Fig. 1.5) like planets that move around the stars, and therefore this model was called planetary model.

The planetary model was greatly inconsistent with Thomson's hypothesis in which the atom is a mixture of positive and negative particles that uniformly mixed throughout the atom. Based on the classical electromagnetic theory, however, the model failed to solve stability problem of the atom as the electrons lose energy and falling into the nucleus under the influence of attraction forces. The model proposed by Rutherford relied heavily on classical physics and was superseded in a few years by the Bohr atomic model, which

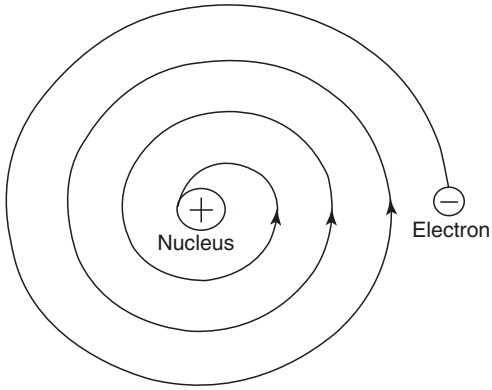

Fig. 1.5 Planetary model: In this model Rutherford proposed that electrons move in circular path around a central positive mass. This was contradicted by the fact that revolution makes electron lose energy while moving in spiral path and fall into the positively charged nucleus under influence of attraction force

incorporated some early quantum theory in combination with some classical concepts.

1.3.2 Bohr Model

In 1913, Bohr introduced a new model to explain atom stability. Bohr model of the atom was the first model that incorporated quantum theory and was the predecessor of wholly quantum-mechanical models. The model focused on electron description and based on spectroscopic observations. Bohr built up his model with the following postulates:

- The electron exists in certain energy levels (stationary states) with circular movement around the nucleus.
- Transition between these stationary states is accompanied with emission or absorption of electromagnetic radiation. The energy difference between these two energy levels is given by

$$\Delta E = \hbar v \tag{1.3}$$

where ħ (i.e. *h* bar) or sometimes reduced plank's constant is commonly associated with angular momentum and given by

$$\hbar = h / 2\pi \tag{1.4}$$

- Quantization of orbit. The only allowed orbits (stationary states) are those for which the angular momentum *L* is

$$L = n\hbar$$

where *n* is principal quantum number and takes values of 1,2,3,….., *n* and cannot be less than one.

Bohr's postulates were experimentally confirmed in experiments of Franck and Hertz (German scientists) in 1913 who studied the inelastic scattering of electrons of mercury atoms. This experiment showed that the energy levels of mercury atom were discrete. However, Bohr's model had no way of approaching non-periodic quantum-mechanical phenomena, like scattering. Furthermore, although Bohr' model served to predict energy levels, it was not able to explain transition rates between levels. Finally, the model was successful only for one-electron atoms like hydrogen and fails even for helium. To correct these drawbacks, one needs to apply a more completely quantum-mechanical treatment of atomic structure, and such an approach is used in Schrödinger theory.

1.3.3 Quantum Mechanics Model

The quantum mechanics model is derived from the quantum theory in which electron location and momentum are governed by the wave function. This hypothesis is denoted as uncertainty principle (Heisenberg principle) and states that the position and momentum of the electron can't be determined simultaneously with the same high precision. Stated another way, the more the precision in determining the electron location, the low the probability of determining the momentum and vice versa. The theory used the term orbitals to describe the location of the electrons, which are volumes in space used to define the probability distribution function. Four quantum numbers were introduced to define the electrons and their orbitals around the nucleus:

1. Principle quantum number (*n*): it is an integer number that indicates electron energy and orbital size, and it is the same number intro-

duced by Bohr. It takes values $n = 0,1,2,\ldots\ldots$, while the maximum number of electrons in certain energy level is equal to $2n^2$.
2. Angular quantum number (l) describes the orbital shape of a particular principal quantum number. It divides energy shells or levels into subshells (sublevels). These sublevels represented by letters like *s*, *p*, *d* and *f*. Angular quantum number takes values $l = 0,1,2\ldots,n-1$.
3. Magnetic quantum number, m_l ($m_l = -l,\ldots, 0,\ldots, +l$) specifies the orientation in space of an orbital of a given energy (n) and shape (l). This number divides the subshell into individual orbitals which hold the electrons; there are $2l+1$ orbitals in each subshell.
4. Spin quantum number, m_s ($m_s = +½$ or $-½$) defines the orientation of the spin axis of an electron. An electron can spin in only one of two directions.

1.4 Structure of the Atom

As mentioned earlier, an atom is the main building block of matter. The atomic mass is concentrated in the nucleus which considered the heaviest portion of the atom. The positively charged nucleus contains particles of nearly equal mass, protons and neutrons, electrically balanced with negatively charged electrons moving in certain orbitals around it. Any element can be represented as

$$\begin{matrix} A \\ Z \end{matrix} X$$

where A atomic mass number is the sum of protons number Z and neutrons number N. The atomic number Z equals also the number of electrons in stable nuclei. It is not applicable to have two different elements having the same atomic number. The periodic table is arranged by order of increasing atomic number, which is always an integer. On the other hand, different forms of the same element can have different masses (i.e. have same atomic number) which are called isotopes, while those that have the same number of neutrons are called isotones. Isobars are nuclide with different numbers of protons and neutrons but with the same mass number. Examples of the three different nomenclatures are described in Table 1.1.

1.4.1 Mass and Energy

Mass and energy were considered two different quantities. Early 1900s, Einstein proved by his equation that neither mass nor energy was conserved separately. Thus, the mass can be converted to energy and vice versa while total mass- energy was conserved. In the following section the conversion of mass and energy will be demonstrated.

1.4.2 Atomic Mass Unit

The first atomic weight was initially proposed by *John Dalton* in 1803 as the mass of the hydrogen atom, H-1. Then it was suggested by *Wilhelm Ostwald* that it can best expressed in terms in units of 1/16 of the weight of the oxygen atom. Atomic mass can be measured by approximating the weight of a proton or neutron which indicates the masses of atom nucleons. The atom mass is expressed by a unified unit called the atomic mass unit denoted by the symbol *u*. In 1961, the international union of pure and applied chemistry had adopted and defined the modern applications of atomic mass unit and related it to the mass of carbon-12.

The definition of the atomic masses has been based on the unified mass scale considering one mole of carbon-12 which by conversion equals 12 g as the best reference nuclide. Determination of ^{12}C atom mass in grams using Avogadro's number divided on the total number of the individual atom nucleons indicates the masses of these nucleons which used to convert one atomic mass unit (1 u) to grams. Therefore, the atomic mass unit is one-twelfth ^{12}C atom in its electronic and nuclear ground state:

Table 1.1 Some examples of isotopes, isobars and isotones

Isotopes	Same Z	$^{16}_{8}O$	$^{17}_{8}O$	$^{18}_{8}O$
		$Z = 8$		
Isobars	Same A	$^{18}_{9}F$		$^{18}_{8}O$
		$A = 18$		
Isotones	Same N	$^{19}_{9}O$		$^{18}_{8}O$
		$N = 10$		

$$1\ \text{u} = \frac{1}{12} m\left({}^{12}_{6}\text{C}\right)$$

$$\text{Thus, mass of one atom of } {}^{12}\text{C} = \frac{12\,\text{g/mol}}{6.022\ 141\ 29\times10^{23}\,\text{atoms/mol}} = 1.992\ 646\ 705\times10^{-23}\,\text{g/atom}$$

$$\text{The mass per nucleon} = \frac{1.992\ 646\ 705\times10^{-23}\,\text{g/atom}}{12} = 1.660\ 538\ 921\times10^{-24}\,\text{g}$$

Then, $1\ \text{u} = 1.660\ 538\ 921\times10^{-27}$ kg.

Now the mass of proton and neutron in terms of atomic mass unit can be determined by using its actual mass in grams:

$$\text{Proton mass}\left(m_\text{p}\right) = \frac{1.672\ 621\ 777\times10^{-27}}{1.660\ 538\ 921\times10^{-27}} = 1.007\ 276\ 467\ \text{u}$$

$$\text{Neutron mass}\left(m_\text{n}\right) = \frac{1.674\ 927\ 351\times10^{-27}}{1.660\ 538\ 921\times10^{-27}} = 1.008\ 664\ 916\ \text{u}$$

Conversion of the energy unit from the SI scale to the unified atomic mass unit is being done by using Einstein's mass-energy relationship ($E = mc^2$ where c is the speed of light in vacuum) taking into account that $1\ \text{eV} = 1.602\ 176\ 565\times10^{-19}$ kg.m^2/s. Inserting this quantity of mass $1\ \text{u} = 1.660\ 538\ 921\times10^{-27}$ into Einstein's equation and applying conversion factors, the nucleons mass equivalent energy can be determined.

$$E = mc^2 \tag{1.4}$$

$$= 1\ \text{u}\left(\frac{1.660\ 538\ 921\times10^{-27}\,\text{kg}}{\text{u}}\right)\times\left(299\ 792\ 458\ \text{m/s}\right)^2\left(\frac{1\ \text{N}}{1\ \text{kg}.\frac{\text{m}}{\text{s}^2}}\right)\left(\frac{1\ \text{J}}{N.m}\right)$$

$$= 1.492\ 417\ 955\times10^{-10}\,\text{J}\left(\frac{1\ \text{MeV}}{1.602\ 176\ 565\times10^{-13}\,\text{J}}\right)$$

$$= 931.494\ 060\ 9\ \text{MeV}$$

Some of the constants and conversion factors used in the above derivations can be found in Table 1.2 which provides a number of useful physical quantities and constants used in converting mass into energy and vice versa.

1.4.3 Binding Energy and Mass Defect

For all nuclei, the mass of the nucleus that have been formed is always less than the total composed

Table 1.2 Summary of several physical quantities and constants in atomic and nuclear scale used in mass-energy conversion

Quantity	Symbol	Numerical value	Unit
Avogadro's number	N_A	6.022 141 29×10^{23}	mol^{-1}
Speed of light in vacuum	C	299 792 458	m/s
Electron volt	eV	1.602 176 565×10^{-19}	J
Atomic mass unit-kilogram relationship	1 u	1.660 538 921×10^{-27}	kg
Atomic mass unit-electron volt relationship	1 u (C^2)	931.494 061×10^{6}	eV
Atomic mass unit-joule relationship	1 u (C^2)	1.492 417 954×10^{-10}	J
electron Volt-atomic mass unit relationship	1 eV/C^2	1.073 544 150×10^{-9}	u
Electron mass Energy equivalent	m_e	9.109 382 91×10^{-31}	kg
	m_e	5.485 799 $094\ 6\times10^{-4}$	u
	$m_e\ C^2$	8.187 105 06×10^{-14}	J
	$m_e\ C^2$	0.510 998 928	MeV
Proton mass Energy equivalent	m_p	1.672 621 777×10^{-27}	kg
	m_p	1.007 276 466 812	u
	$m_p\ C^2$	1.503 277 484×10^{-10}	J
	$m_p\ C^2$	938.272 046	MeV
Neutron mass Energy equivalent	m_n	1.674 927 351×10^{-27}	kg
	m_n	1.008 664 916 00	u
	$m_n\ C^2$	1.505 349 631×10^{-10}	J
	$m_n\ C^2$	939.565 379	MeV

Source: NIST (2010 CODATA recommended values)

masses of the contributing nucleons. This is due to conversion of that mass difference to the required energy for holding these nucleons together (i.e. the conversion of mass to binding energy). This mass difference is known as the mass defect and represents the binding energy which is defined as the amount of energy that need to be supplied to a nucleus to completely separate its constituent nucleons. The mass defect can be calculated by adding up the masses of the constituent particles and then subtracting the known mass of that atom:

$$\Delta m = \left[Z\left(m_{\text{proton}} + m_{\text{electron}}\right) + \left(A - Z\right) m_{\text{neutron}} \right] - m_{\text{atom}} \tag{1.5}$$

where:

Δm = mass defect (u)

m_{proton} = mass of a proton

m_{electron} = mass of electron

m_{neutron} = mass of neutron

m_{atom} = mass of the nuclide

Z is the atomic number and A is the mass number.

Since 1 u is equivalent to 931.5 MeV of energy as calculated in Sect. 1.4.2, the binding energy can be calculated by

$$\text{B.E.} = \Delta m \left(\frac{931.5\ \text{MeV}}{1\ \text{u}} \right)$$

Example

Calculate the mass defect of ^{235}U provided that the mass of the atom is 235.043 9 u?

Solution:

The atomic number of the ^{235}U is 92. The mass defect can be calculated by using Eq. 1.5.

$$\Delta m = \left[Z\left(m_{\text{proton}} + m_{\text{electron}}\right) + \left(A - Z\right) m_{\text{neutron}} \right] - m_{\text{atom}}$$

$$\Delta m = \left[92\left(1.007\ 28 + 5.485\ 79\times10^{-4}\right) + \left(235 - 92\right)1.008\ 66 \right] - 235.043\ 9$$

$$= 1.914\ 71\,\text{u}$$

1.4.4 Nuclear Stability

Since Earth formation, there were about 275 stable nuclides found in nature, and more than 2000 nuclides are known to be unstable (i.e. radioactive). The constituents of the unstable nuclei are not arrayed in the lowest potential energy states; therefore, the nucleus undergoes spontaneous decay with time in such a way that this excess energy is emitted forming new nuclide. A study of the characteristics of the naturally stable nuclides provides clues of instability factors of the radioactive nuclides. An *N*/*Z* diagram of the 'line of stability' relates the naturally stable nuclides extending from $Z=1$ for hydrogen up to $Z=83$ for ^{209}Bi to those radioactive according to their neutron and proton numbers. Very long-lived nuclides are shown at the end of the line of stability although of their instability.

A major measure of nuclear stability is the neutron-proton ratio, as a result of the coulomb repulsion and exchange forces between them. Referring to Fig. 1.6 and closer look into light nuclei, the line of stability shows that neutron and proton numbers are equal ($N \approx Z$). For heavy nuclei, the coulomb repulsion between the protons is substantial, and extra neutrons are needed to supply additional binding energy to hold the nucleons together. Thus, the line of stability shows $N \approx 1.5\ Z$, that is heavy stable nuclides have nearly 50% more neutrons than protons. From $Z>83$ all heavier nuclides are unstable. Radioactive nuclides surround the line of stability; nuclides lying above the line are said to be

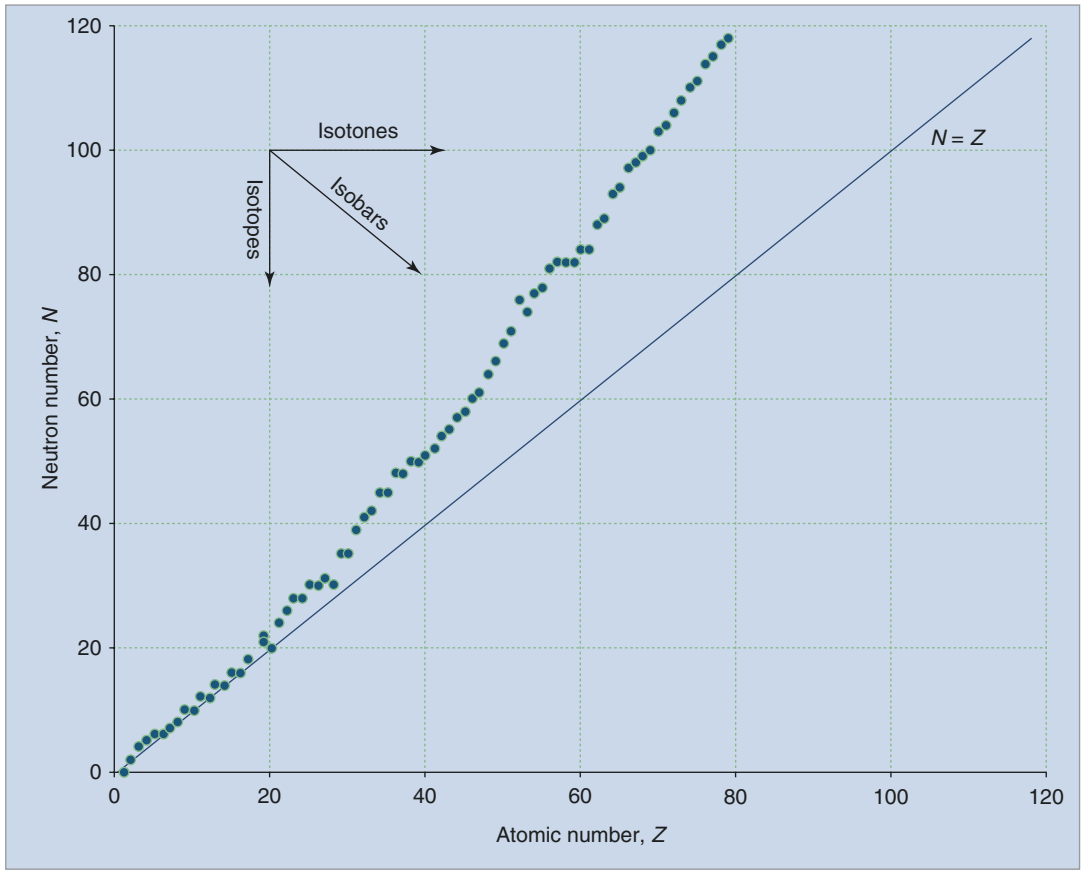

Fig. 1.6 Neutron number (*N*) versus atomic number (*Z*) for nuclides found in nature. The deviation of the stable nuclei from the line of identity (i.e. $Z=N$) is obvious and has been attributed to an increase in neutron number to moderate proton repulsion

'proton deficient', whereas nuclides lying below the line are 'neutron deficient'. Radioactive nuclei attempt to reach the stability by different modes of radioactive decay which is going to be discussed later. In the *N*/*Z* diagram (Fig. 1.6), the excess-neutron number is seen as the vertical distance between the stable nuclides and the diagonal $N=Z$ line. From the frequency distribution of stable isobars, isotopes and isotones, it has been concluded that even numbers of identical nucleons are more stable than odd numbers of the same nucleons (oddness of both *Z* and *N* tends to lower the nuclear binding energy).

1.5 Production of Radiopharmaceuticals

Nuclear medicine is a unique medical specialty that uses radiopharmaceuticals for diagnostic or therapeutic purposes. The diagnostic role is to interrogate valuable functional information about disease biochemistry not only on the cellular or subcellular level but also extend to extract molecular and genetic information. The other good facet of nuclear medicine is its ability to target but treat critical diseases using therapeutic radionuclides. Diagnostic radiopharmaceutical is a radioactive drug that is administered in a tracer quantity with no pharmacological effect on human body. Radiopharmaceuticals can be broadly classified into two different categories, single photon emitters that are commonly used in conventional gamma camera imaging examinations and positron emitter-based radiopharmaceuticals. The former class of compounds are commonly labelled with ^{99m}Tc solution eluted from molybdenum-99 generators. Radionuclides such as ^{201}Tl, ^{67}Ga, ^{111}In-, ^{123}I and ^{131}I belong also to the same class and have several diagnostic or therapeutic applications.

The other class of radiopharmaceuticals are based on labelling with positron emitters (such as ^{18}F, ^{11}C, ^{13}N, ^{15}O, etc.) and used in PET imaging applications such as oncology, cardiology and neurology. These kinds of radiotracers require medical cyclotrons and other essential infrastructures that include radiochemistry production facility, analytical and quality control equipments and other radiation detection and measurements devices. More details about medical cyclotron will be discussed later.

Since naturally occurring radioisotopes are relatively long half-lived and not handled well with human body, an artificially produced radioisotope which is cyclotron or reactor produced is being used. However, on-site radionuclide production is often required for positron emitter radionuclides with short half-lives such as ^{15}O (2.04 min), ^{13}N (10 min) and ^{11}C (20.38 min) which requires a local production to avoid loss of the material due to continuous decay. Since the radioisotopes need to be incorporated into some form of pharmaceutical, it should also be capable of being produced in a form which is amenable to chemical, pharmaceutical and sterile processing.

In March 2000, the fluorine-18-labelled glucose or F-18 fluoro-2-deoxyglucose (F-18 FDG) received Food and Drug Administration FDA approval for usage to evaluate and diagnose oncology patients although the first production was in 1978 for neurological applications. It is worth mentioning that first applications of FDG were focused on neurology and cardiac imaging, but its importance in oncology was realized on a later stage. F18-FDG limitations such as low specific targeting in PET imaging were an incentive for development of new PET tracers with special targeting capabilities. Newly developed PET traces are more specific and allow for imaging biological processes, such as angiogenesis, hypoxia, proliferation, apoptosis and many others. The expression of different receptors can be visualized like the somatization receptor 2, gene expression and dopamine and serotonin receptors in addition to large spectrum of potential cellular and molecular targets. Some of these approaches have found their way forward to the clinic, while others are still under extensive research and clinical evaluation.

1.5.1 Reactor Production Using Neutrons

Artificially produced radionuclide takes place in nuclear reactor by means of fission reaction or by using neutron flux to activate special target

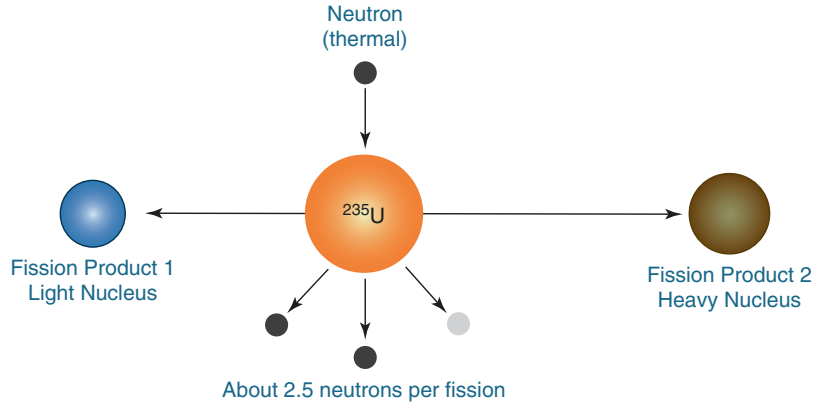

Fig. 1.7 Spontaneous fission reaction; ^{235}U splits into two fission nuclei accompanied with neutrons release which in turn induce another fission reaction (chain reaction initiation)

material located in reactor core. Naturally occurring radioactive material especially heavy nuclei (^{235}U) undergoes spontaneous fission reaction; see Fig. 1.7. The result of such a reaction is two lighter fission fragments and few fission neutrons in addition to large amount of energy released. The fission neutrons will in turn initiate further fission reaction or what is called chain reaction. As the reactor uses the newly generated neutrons to keep fission reaction going on, on average one fission neutrons induce one more fission, so the process is self-sustaining chain reaction.

Since *N*/*Z* ratio is high for fission fragments, it will undergo β^- decay until either stable nuclei are reached or relatively long half-life nuclide is reached and extracted from the reaction. The most important isotope produced in this way is ^{99}Mo which decays into ^{99m}Tc through β^-decay with half-life 2.75 days. The daughter nuclide (^{99m}Tc) has very important clinical value in nuclear medicine and in wide variety of diagnostic examinations. The production of ^{99}Mo by a fission reaction is represented as $^{235}U\ (n, f)\ ^{99}Mo$.

In this reaction, uranium/aluminium alloy (containing uranium enriched to 45 % ^{235}U) is used as target material. The typical yield of ^{99}Mo is in the order of (4–10 Ci) per g of ^{235}U irradiated for 50–200 h in a neutron flux of 1.5×10^{14} n cm^2 s^{-1}.

Molybdenum-99 production can also take place through neutron activation in which target material (MoO_3) is irradiated by neutron flux (n, γ) reaction for 1 week.

$$^{98}\mathrm{Mo}(n,\ \gamma)^{99}\ \mathrm{Mo}$$

$$^{98}_{42}\mathrm{Mo} + {}^{1}_{0}n \rightarrow {}^{99}_{42}\mathrm{Mo} + \gamma$$

In this method of production, yield depends on neutron flux, neutron energy, target material and reaction activation cross section. Radionuclides production by (n, γ) reaction having poor specific activity as the produced nuclide and target material are isotopes and cannot be chemically separated. Other radionuclides used for diagnostic and therapeutic application in nuclear medicine such as^{131}I, ^{153}Sm, ^{90}Y, ^{89}Sr, etc., are reactor produced.

1.5.2 Accelerator Production Using Charged Particles

Charged particle (protons, deuterons and alpha particles) accelerated by means of particle accelerator should possess sufficient kinetic energy to penetrate coulomb repulsion forces surrounding the nucleus. In this kind of radionuclide production, electrically charged particles are being accelerated to very high energy in range of MeV and then extracted towards target material initiating nuclear reaction for certain period of time in order to obtain sufficient amount of radionuclide. Radionuclide production takes place in charged particle accelerator by different nuclear reactions. The (p, n) reaction is one of the most reactions used for this purpose where irradiated atoms gain one proton accompanied by emission of neutron. The most common example is the production of F-18 from heavy water as shown here:

$$^{18}_{8}\mathrm{O}\left(p,n\right)^{18}_{9}\mathrm{F}$$

Another common nuclear reaction used is (*d*, *n*) in which the target nucleus will catch the accelerated particle (deuteron), subsequently the produced radionuclide atomic number and mass number each increases by one. The (*d*, *n*) reaction is given by:

$$^{A}_{Z}X\left(d,n\right)^{A+1}_{Z+1}X$$

An example of a radionuclide that is produced by deuteron irradiation is oxygen-15, and this reaction is written as

$$^{14}\mathrm{N}\left(d,n\right)^{15}\mathrm{O}$$

There are many different types of particle accelerator including the Van de Graaff accelerator, cyclotron, synchrocyclotron, synchrotron and linear accelerator although they are different types, but the main concept is still the same. Charged particles are accelerated in the presence of electric or magnetic field or both to reach the desired energy for extraction towards its target. Charged particle accelerators can produce radionuclides with high specific activity than reactor did.

1.5.2.1 Medical Cyclotrons

The first medical applications of cyclotron start at the University of California, Berkeley, when Lawrence and his brother John quickly demonstrated the clinical importance of cyclotron-produced radioisotopes in disease research. In 1936, they started to produce radioactive phosphorus for leukaemia and polycythaemia treatment. These were the first therapeutic applications of artificially produced radioisotopes on human patients.

By 1938, the Berkeley 27 in. (later upgraded to 37 in.) cyclotron had produced ^{14}C, ^{24}Na, ^{32}P, ^{59}Fe and ^{131}I radioisotopes, among many others that were used for medical research. Nowadays medical cyclotrons widely use medium energy 10–20 MeV for routine production of positron emitters (^{18}F, ^{11}C, ^{13}N, ^{15}O,…) for synthesis of radiopharmaceuticals used in diagnostic purposes. Other commercially available medical cyclotrons (Fig. 1.8a) are in energy range 18–24 MeV for traditional positron emitters production as well as for single photon emitters production (^{123}I, ^{111}In, ^{67}Ga, ^{57}Co, ^{99m}Tc) as diagnostic biomarkers and other applications in SPECT imaging.

Cyclotron first designed to accelerate the positive ions H^+ and $^2H^+$, but after that cyclotron design changed to accelerate negative ions hydrogen or deuteron. Positive ion cyclotron acceleration does not need as much vacuum as negative ion cyclotron acceleration, but it results in cyclotron metal part activation, and it has complicated extraction beam system which became more simple in negative ion cyclotrons giving the flexibility to use dual beam production with similar or different beam currents.

The cyclotron consists of a large cylindrical chamber placed between the poles of a huge electromagnet. The magnet system consists of magnet itself, magnet poles made of low-carbon steel and magnet coils made of hollow copper conductors. Inside the chamber, two big hollow D-shaped copper electrodes (Dees) are connected to a very high voltage oscillating with high radio frequency in range of 20–30 MHz and an ion source located at the centre of chamber where the ionization process of hydrogen or deuteron gas takes place. The radio-frequency (RF) system (particle acceleration) includes RF generator, RF cable and RF cavity. The chamber is kept under very high vacuum (e.g. 10^{-07} mbar) by means of vacuum system (e.g. diffusion and mechanical pump).

The cyclotron operation takes place through a master PC station which allows an operator to set up irradiation parameters (beam current and irradiation time) and have a control over many of the cyclotron operations and functions overseeing the production process step by step in a diagrammatic manner. Some of these parameters to be followed are ion source, target, foil and probe currents, Dee voltage, gas flow and other critical RF settings as well as helium cooling pressure. Ionization starts as high purity gas (H_2, D_2) that pass through the ion source with predefined flow rate. Ionization

Fig. 1.8 Medical cyclotron for radiopharmaceuticals productions. (**a**) ACS cyclotron TR-24 (24 MeV) high current cyclotron for production of PET and SPECT radionuclides (Courtesy of ACS, Inc.). (**b**) GE PETtrace 800 series medical cyclotron (16.5/8.4 MeV) (Courtesy of GE Health Care). (**c**, **d**) are their respective Dee's system

of such gas is then followed by injection of ionized particles into the chamber centre between the Dees where constant magnetic field is applied along ionized particle path. The role of applied magnetic field during particle acceleration is to focus on and maintain accelerated particle in spiral path (for explanation, see Fig. 1.9). The force of applied magnetic field is given by

$$F = qvB \tag{1.6}$$

And the centripetal force can be described as

$$F = \frac{mv^2}{r} \tag{1.7}$$

where B magnetic field strength is in Tesla, r particle's radius in metre, q particle's charge in coulomb and m particle's mass in kg. From Eqs. 1.6 and 1.7,

$$qvB = \frac{mv^2}{r} \tag{1.8}$$

Hence, particle velocity v is represented by

$$v = \frac{qBr}{m} \tag{1.9}$$

And particle frequency in spiral path is $f = \frac{v}{2\pi r}$, substitute for v so

$$f = \frac{qBr}{2\pi rm} \tag{1.10}$$

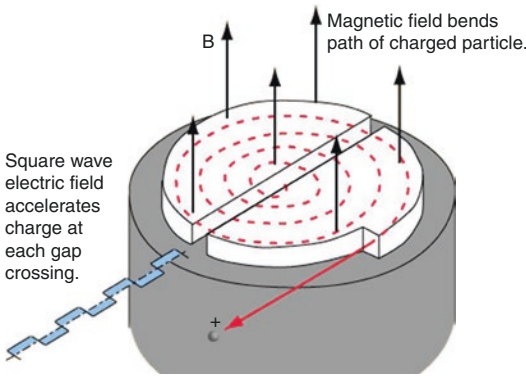

Fig. 1.9 Schematic diagram showing particle path in a cyclotron as well as the applied magnetic and electric field. Ion source located at the centre of high-vacuum chamber, negative ions being maintained by magnetic field accelerated by RF until reach extraction radius then directed to the target body by thin carbon foil (From http://hyperphysics.phy-astr.gsu.edu/hbase/hph.html)

Hence,

$$f = \frac{qB}{2\pi m} \tag{1.11}$$

At resonance condition between the high-frequency electric field (RF) and the circular motion frequency

$$f = f_{\text{oscillator}} \text{ or } qB = 2\pi \text{mf}_{\text{oscillator}}$$

Under resonance condition, as the particle completes half revolution, the polarity of the field will change. The particle will again be accelerated across the gap; its velocity will increase so that now it will move in a circular path of greater radius, but its frequency will not be affected and the process of acceleration continues. Hence, the maximum kinetic energy achievable by the accelerated particle is given by

$$E = \frac{1}{2}mv^2 \tag{1.12}$$

Using Eq. 1.9 to substitute for v in Eq. 1.12.

$$E = \frac{B^2 r^2}{2}\left(\frac{q^2}{m}\right) \tag{1.13}$$

Once the required kinetic energy is gained by the accelerating particles, the positively charged ions (H^+ and $2H^+$) are extracted by means of a stripping foil technique in which thin carbon foil is placed at the extraction radius to strip electrons as the negatively charged accelerated ions passing through it (Fig. 1.10). Subsequently, the direction and curvature of the positively charged beam path change (opposite direction) towards the selected target, and bombardment starts for radionuclide production.

The target system where the bombardment and nuclear reactions takes place can be liquid, gas or solid target. Heat dissipation on the target should be removed by means of cooling applied by water cooling system and high purity helium gas. At the end of bombardment, the activity will transfer to specific synthesis modules where the chemical reaction and labelling under preset conditions of temperature and pressure take place to have the final radiopharmaceuticals.

1.5.3 Specific Activity

Specific activity is defined as activity per unit mass of the radioisotope (mCi/g, Bq/mol) including radioactive and nonradioactive molecules. Since one mole of any element contains Avogadro's number of atoms, so for calculation standardization, it is good to represent specific activity in unit activity/mol. Specific activity has an important role in PET radiopharmaceuticals because of possible competition between cold and radioactive molecules with noticed uptake reduction in different tissue.

1.5.4 Saturation Yield

Saturation yield of radionuclide production is represented as the maximum activity produced per unit microampere (mCi/μA), and it is given by:

$$\left(\text{mCi}/\mu\text{A}\right) = \frac{A_0}{I\left(1-e^{\lambda t}\right)} \tag{1.14}$$

where A_0 is activity (mCi) at the end of bombardment (EOB), $\left(1-e^{\lambda t}\right)$ is saturation factor, t is irradiation time in minutes, λ is decay constant of

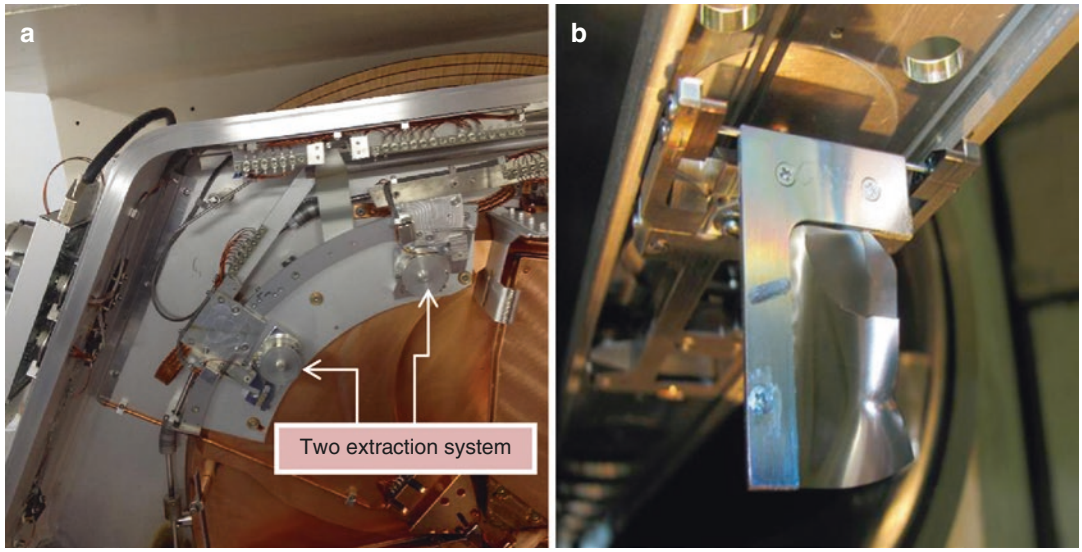

Fig. 1.10 Cyclotron extraction system. (**a**) GE PETtrace 800 extraction system. One extraction system for each target set allowing dual beam production (Courtesy of GE Health Care) and (**b**) used and cracked extraction foil (From www.triumf.ca)

isotope of interest and I is the beam current in (μA).

Saturation factor is defined as the production rate of isotope during irradiation time of the target for a time t. Saturation factor approaches unity within 5–7 half-lives of irradiation time of radionuclide produced. At that point, equilibrium between production rate and decay occurs.

The above equation is valid for thin target while there is no beam attenuation. For thick target (beam is completely absorbed in the target) where there is variations in beam energy because of gradual energy loss due to interactions of charged particles with electrons, target yield depends on other factors such as energy and stopping power, and it is given by:

$$Y = \frac{1.03 \times 10^5}{Z \times A} \int_{E_{in}}^{E_{out}} \frac{\sigma(E)}{dE/dX} dE \quad \text{for } t >> T_{1/2}$$

where Y is the thick target yield (μCi/μA), Z atomic number of charged particle, A mass number of target nuclei, dE/dX stopping power of charged particle in MeV/g, $\sigma(E)$ cross section in mbarn, t irradiation time, $T_{1/2}$ half-life of isotope, E_{in} incident energy of the particle and E_{out} exiting energy of the particle.

1.6 Radioactivity

As mentioned previously, all heavy (large) nuclei (i.e. $Z>83$) are structurally unstable (unstable nucleus) and therefore radioactive. Sooner (nanosecond) or later (thousands of years), those unstable nuclei change to more stable nuclear configurations through various processes of spontaneous radioactive decay that involve emission of energetic particles such as alpha, beta and gamma. Thus, unstable radionuclide (parent) transforms to more stable nuclide (daughter) throughout various radioactive decay modes that will be discussed in the following sections.

1.6.1 Modes of Decay

1.6.1.1 Alpha Decay

Alpha particle ($^4_2$He) is the nucleus of the helium atom and consists of two protons and two neutrons. From the stability standpoint, the alpha particle has very stable configurations and plays an important role in reducing the heavy weight of some radioactive nuclei transforming them into less excited or ground state. The position of those radionuclides on the N/Z diagram determines its mode of

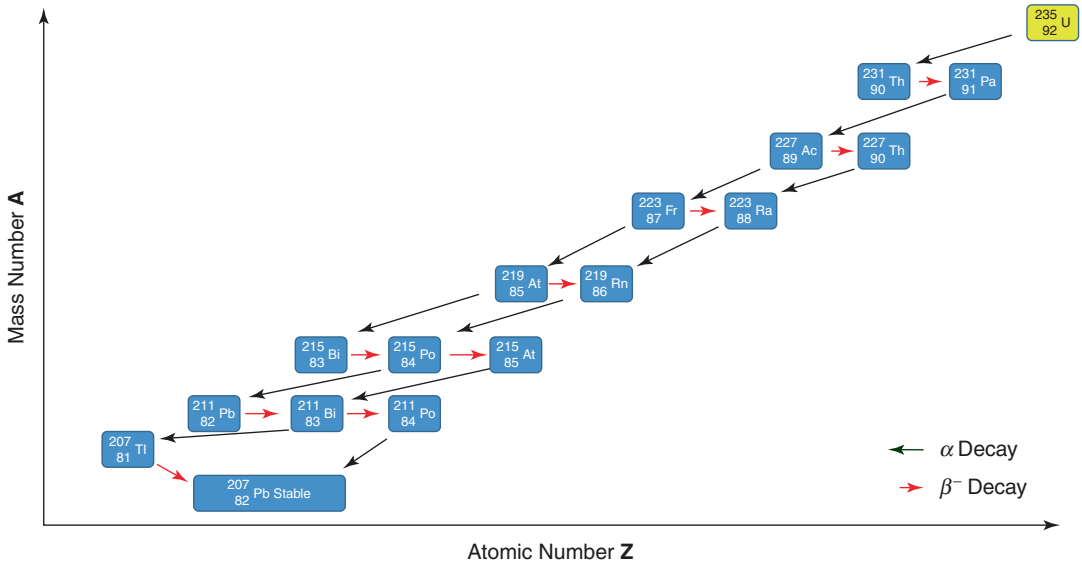

Fig. 1.11 ^{235}U decay series: unstable ^{235}U decays to stable ^{207}Pb nuclei through alpha and beta decay modes

radioactive decay; for heavy large nuclei (Z>83), they need to reduce their A, Z and N numbers to reduce large mass and charges to achieve the stability through the emission of several helium-4 nucleus ($^4_2$He nuclei – alpha particle). Each emission of alpha particle reduces the mass by 4; some heavy radionuclides (^{235}U) reach its stability through a chain of transformation that need several alpha particle emission (decay series) before a stable nuclide (^{207}Pb) is achieved. The decay series of such a transformation can be seen in Fig. 1.11; the decay modes include those leading to ejection of an alpha particle (α) or a beta particle (β^-).

Radium-226 is a typical example of alpha decay; see decay scheme in Fig. 1.12.

$$^{226}_{88}\mathrm{Ra} \rightarrow {}^{222}_{86}\mathrm{Rn} + {}^{4}_{2}\mathrm{He} + 4.87\ \mathrm{MeV}$$

Although the alpha particles are monoenergetic and their kinetic energy is below 10 MeV (in range 4–9 MeV), it can penetrate the parent nucleus coulomb barrier of 30 MeV due to quantum-mechanical effect of tunnelling (tunnelling through the barrier).

1.6.1.2 Beta Minus (β^-) Decay

Small radionuclide (Z<83) of unstably high N/Z ratio indicates an excess of neutrons (proton deficient), lie above the line of stability. Beta minus

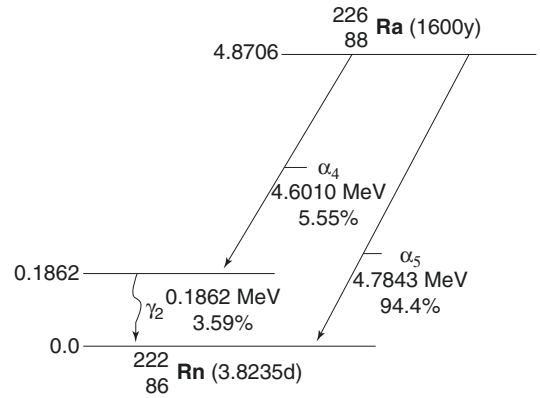

Fig. 1.12 ^{226}Ra decay scheme

decay transforms a neutron into a proton and eject one electron (beta particle) plus antineutrino, leading those nuclei closer to the line of stability by adding more positive charge (charges increase on the nucleus and a slight reduction of mass), thus, changing only the atomic number Z of the parent by one unit (+1) leaving the atomic mass A constant (isobar daughter).

$$n \rightarrow p + \overline{e} + \overline{\nu_e}$$

$$^{A}_{Z}P \rightarrow {}^{A}_{Z+1}D + \overline{e} + \overline{\nu_e}$$

Unlike the alpha particles (monoenergetic), the beta particles are being emitted with a range of

energies (MeV) forming a continuous spectrum (not all the beta particles being emitted with the same energy value); some of them reaches a maximum energy denoted by $E_{\beta max}$, whereas others are emitted with smaller energy. Thus, the energy released from this transformation is distributed randomly between the electron (beta particle) which has most of it and the antineutrino.

There are some radionuclides of medical interest that undergo decay solely by β^- emission (^{3}H, ^{14}C, ^{32}P and ^{90}Y) or combination of (β^-, γ) emission (^{131}I, ^{133}Xe and ^{137}Cs). Radionuclide can be used either as diagnostic radiopharmaceuticals or as therapeutic products. Pure beta-emitting radionuclides (e.g. Yettrium-90, ^{90}Y) are mainly used with therapeutic purposes, to deliver high-dose rate on tumours due to their high linear energy transfer (LET) and range of deposition in tissue several mm to cm.

^{90}Y is one of the radionuclides that is most widely used in nuclear medicine therapeutic applications. Thanks to its long β particle range, ^{90}Y allows a uniform irradiation of large tumours commonly expressing heterogeneous perfusion and hypoxia. The average energy of β^- emissions from ^{90}Y is 0.9367 MeV and maximum of 2.27 Mev (see Fig. 1.13, ^{90}Y decay scheme), with a mean tissue penetration of 2.5 mm and a maximum of 11 mm. However, ^{90}Y-labelled SIR –microspheres (diameter ~30 μm) are used in selective internal radiation therapy for the treatment of hepatocellular carcinoma (HCC) and potentially other diseases metastatic to the liver. ^{131}I radionuclide is being used in both diagnostic and therapy (combination of emission); it is used for the treatment of variety of thyroid disorders, benign and malignant. The decay scheme for ^{131}I indicates emission of six beta minus particles of varying energies and emission of 14 gamma rays of different energies. Thus, 90 % of the tissue damage from ^{131}I is caused by beta particles due to the LET rate for beta minus particles, which is much higher than for gamma rays.

1.6.1.3 Positron (β+) Decay

Proton-rich radio nuclei (lie below the line of stability) achieve their stability by a nuclear change which requires either a positive charged electron emission (positron decay) or a capture of orbital electron (electron capture). Radioactive transformation by positron (β^+) emission is occurred by rearrangement of the protons and neutrons of the nucleus binding in a way they could supply the essential energy ($E = 1.022$ MeV) for this transformation which yield a neutron, create positive electron and eject a neutrino and reducing the atomic number by one. The energy 1.022 MeV is being consumed in producing two electron masses as a product of the decay (Fig. 1.14).

$$p \rightarrow +e^+ + v_e$$
$$^A_Z P \rightarrow {}^A_{Z-1} D + e^+ + v_e$$

An example of (β^+) decay:

$$^{18}_{9}\mathrm{F} \rightarrow {}^{18}_{8}\mathrm{O} + {}^{0}_{1}e + v + Q + \text{orbital electron}$$

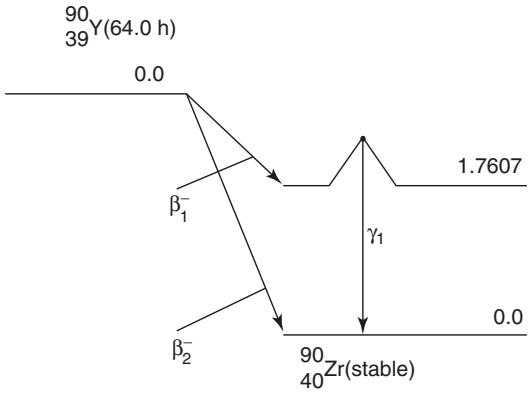

Fig. 1.13 ^{90}Y decay scheme

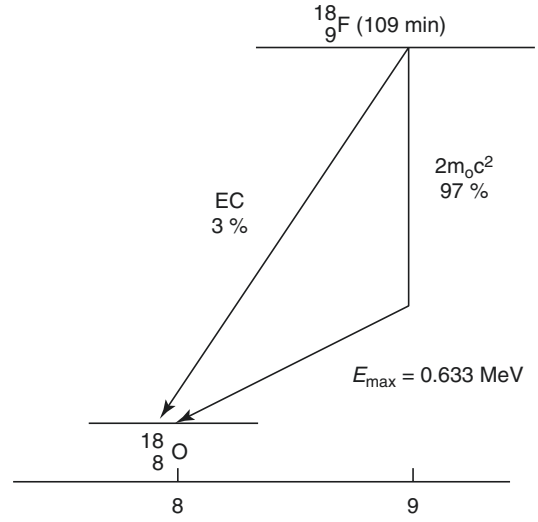

Fig. 1.14 ^{18}F decay scheme

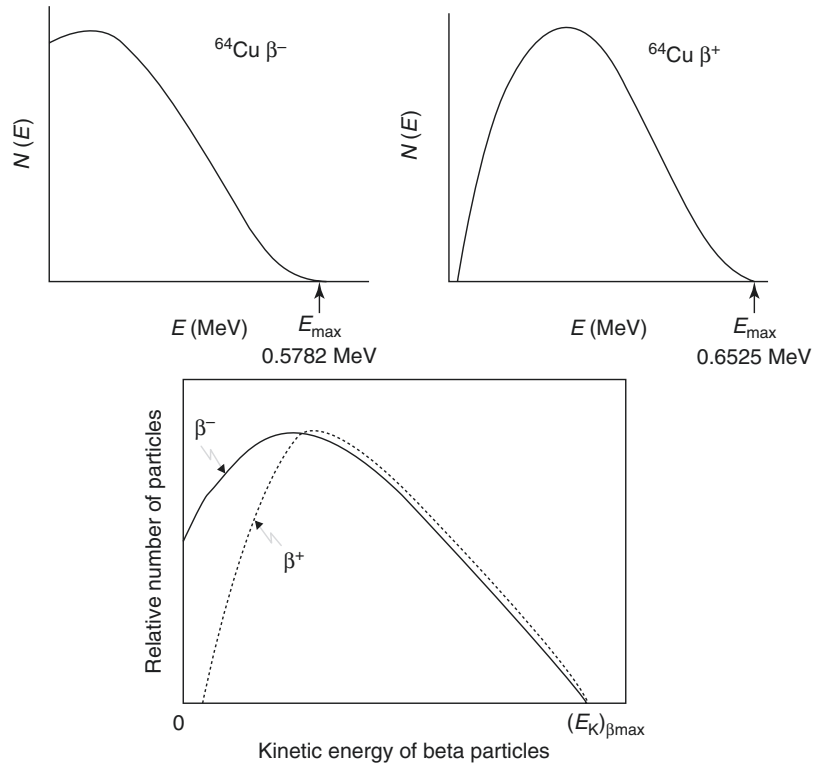

Fig. 1.15 Beta particles energy spectrum for $^{64}_{29}Cu$ undergoing β^- (*top left*) and β^+ (*top right*) emissions with maximum energy 0.579 and 0.653 MeV to reach stable nuclides $^{64}_{30}Zn$ and $^{64}_{28}Ni$, respectively (Adapted from Martin James [3]). Difference in energy spectrum of beta minus and beta plus is also shown in the bottom figure (Adapted from Podgorsak [23])

Similarly to beta minus, the beta plus is continuously distributed in an energy spectrum skewed to the right as shown in Fig. 1.15 (charge effects cause shift to higher energies).

The average energy $\overline{E_\beta}$ of the spectrum is approximately one-third of the end point energy (maximum energy $E_{\beta\ max}$); the general relationship for the average kinetic energy of the beta particles is:

$$\overline{E_{\beta^+}} = \frac{1}{3} E_{\beta^+\ max} \times \left(1 + \frac{\sqrt{E_{\beta^+\ max}}}{4} \right) \quad \text{for } \beta^+ \text{ decay} \tag{1.15}$$

$$\overline{E_{\beta^-}} = \frac{1}{3} E_{\beta^-\ max} \times \left(1 - \frac{\sqrt{Z}}{50} \right) \left(1 + \frac{\sqrt{E_{\beta^-\ max}}}{4} \right) \quad \text{for } \beta^- \text{ decay} \tag{1.16}$$

where $\overline{E_{\beta^-}}$ and $\overline{E_{\beta^+}}$ are in MeV.

1.6.1.4 Electron Capture (EC)

As mentioned earlier, the proton-rich nuclei undergo radioactive transformation indicated by capture of orbital electron. This happens when the sufficient energy is not available for positron emission ($E < 1.022$ MeV); the only way to reduce number of protons in proton-rich nuclei would be the capture of an orbital elec-

tron. Due to de Broglie wave pattern of the orbiting electrons, they could come close to or pass through the unstable nucleus allowing capture to occur yielding Z reduction by 1, N increase by 1, and the mass number A remains the same. The capture from the close atom shells (K with 90 % capture probability, L (10 %) and M (1 %)) leaves vacancy which then filled by a higher energy level electron, and characteristic radiation is emitted with probability of Auger process; for more details, refer to Sect. 1.7.1.

^{55}Fe is a radionuclide undergoes such a transformation to reach the nuclear stability.

$$p + \bar{e} \rightarrow n + \nu_e$$
$$^{A}_{Z}P + \bar{e} \rightarrow {}^{A}_{Z-1}D + \nu_e$$
$$^{55}_{26}\mathrm{Fe} + {}^{0}_{-1}e \rightarrow {}^{55}_{25}\mathrm{Mn} + \nu + Q$$

Although positron emission occurs more frequently among light elements and electron capture among heavier elements, unstable nucleus has energy of $E \geq 1.022$ MeV and reaches stability by positron emission accompanied with electron capture mode of decay. ^{11}C and ^{18}F are radionuclides of medical interest that undergo such competitive decay (β^+ and EC). See Fig. 1.16.

1.6.1.5 Isomeric Transition

Most of radioactive decay yields a daughter nucleus in an excited state relieved in less than 10^{-9} s by gamma emission. However, some daughter nuclei may be formed in excited states that could exist long enough to be measurable.

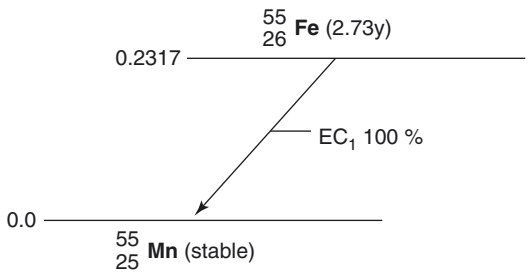

Fig. 1.16 $^{55}_{26}Fe$ decay scheme illustrates positron emission accompanied with electron capture

Such a "long-lived" excitation represents a metastable (or isomeric state). To relieve the excitation energy of that state, emission of gamma rays is carried out. An example of such decay is the production of ^{99m}Tc by radioactive transformation of ^{99}Mo; see Fig. 1.17 ^{99}Mo decay chain. ^{99m}Tc is decayed considerably with almost 6 h half-life, and it is relieved to the ground state of ^{99}Tc throughout the gamma ray emission.

1.6.2 Radioactive Decay Equations

The fundamental law of radioactive decay is based on the fact that the decay, i.e. the transition of a parent nucleus to a daughter nucleus is a purely statistical process. The disintegration (decay) probability is a fundamental property of an atomic nucleus and remains equal in time.

Mathematically this law is expressed as

$$dN = \lambda N.dt$$
$$\lambda = \left(-dN/dt\right)/N$$

where λ is the decay constant and it is unique value for each radioisotope.

$(-dN/dt)$ is the disintegration rate, and the negative sign signifies that N is decreasing with time. N is the number of radioactive nuclei. By integration and applying the boundary conditions in the beginning, $t=0$ and $N=N_0$, we obtain

$$\ln\left(\frac{N}{N_o}\right) = -\lambda t$$

Subsequently the equation of exponential decay

$N=N_o\, e^{-\lambda t}$

Or in terms of activity

$$A = A_o e^{-\lambda t} \tag{1.17}$$

Half-life time ($t_{1/2}$) is the time required for radioactivity to reach half of its original value and is related to the decay constant through the relation:

$$T_{1/2} = 0.693 / \lambda \tag{1.18}$$

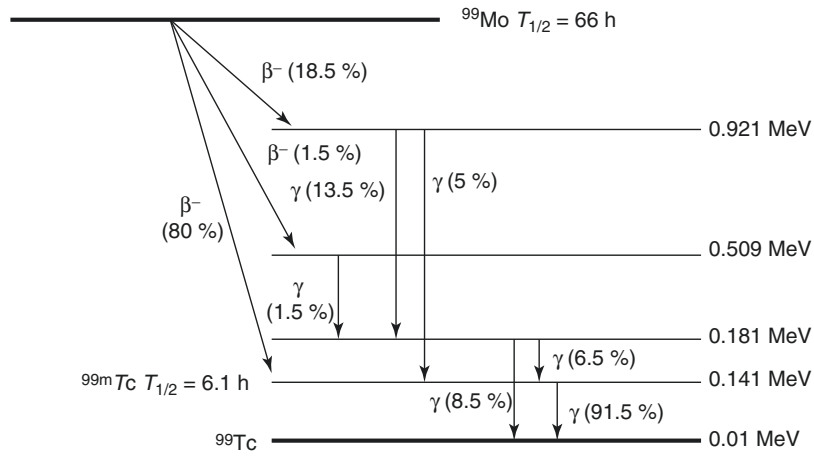

Fig. 1.17 ^{99}Mo decay scheme, 80 % of ^{99}Mo undergoes beta minus decay to reach metastable technetium-99 which disintegrates to stable technetium-99 through emission of 140 keV gamma rays

This can be easily derived if we substitute the activity A or number of atoms N by (½)A or (½)N receptively in the two equations above while denoting $t = T_{1/2}$.

1.7 Interaction of Radiation with Matter

Ionizing radiation either heavy or light charged particles or electromagnetic waves (such as gamma rays, x-rays, etc.) do interact in different modes with matter. Energetic charged particles interact with matter by losing kinetic energy via excitation and ionization. Excitation and ionization occur when charged particles lose energy by interacting with orbital electrons. Excitation is the transfer of some of the incident particle's energy to electrons in the absorbing material, rising electron to higher energy level. In excitation, the energy transferred to an electron does not exceed its binding energy. Following excitation, the electron loses energy going to its original energy level, with the emission of the lost excitation energy in the form of electromagnetic radiation or Auger electrons. If the transferred energy exceeds the binding energy of the electron, then ionization occurs in which the electron is ejected from the atom.

Sometimes the ejected electrons possess sufficient energy to produce secondary ionization. Light charged particles as positrons during passing through absorbing material lose their energy due to interaction with electrons of absorber atoms and come to almost rest; recombination of positron and electron will initiate annihilation process. Photon detection of the annihilation process is the basis upon which PET imaging has been conceptualized.

1.7.1 Photoelectric Effect

In the photoelectric effect, all of the incident photon energy is transferred to the inner most electron of the absorber, which is ejected from the atom. The kinetic energy of the ejected electron (E_e in Eq. 1.19) is equal to difference between incident photon energy (E_i) and binding energy of the orbital electron (E_b) (Fig. 1.18a). Therefore, for photoelectric interaction to occur, the energy of incident photon should be equal to or slightly above the binding energy of ejected electron. As a result of this interaction, the atom becomes unstable and ionized with vacancy in the inner most energy shell. Subsequently, electron from higher energy level will fill this gap with emission of characteristic x-ray (K, L, M, etc.). Alternatively, the emitted radiation due to electron transition may result in bombarding an orbital electron in the same atom producing what is called Auger electron, named after one of the discoverers Pierre Victor Auger (Fig. 1.18b).

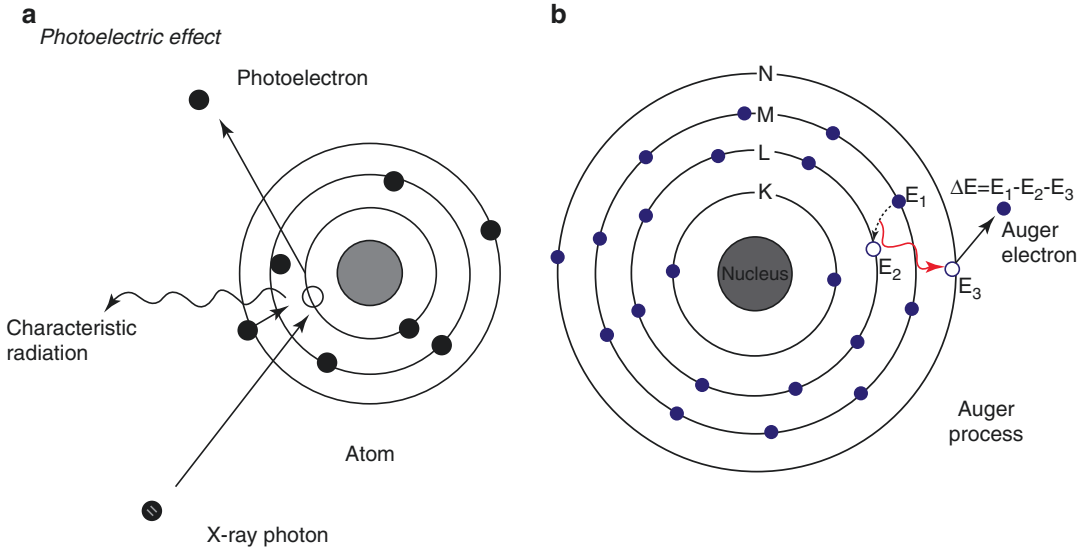

Fig. 1.18 Photoelectric effect and Auger electron process. (**a**) Photoelectric interaction; gamma rays interact with most inner shell; energetic electron is ejected with energy equal to difference between incident photon energy and K-shell binding energy and (**b**) Auger electron

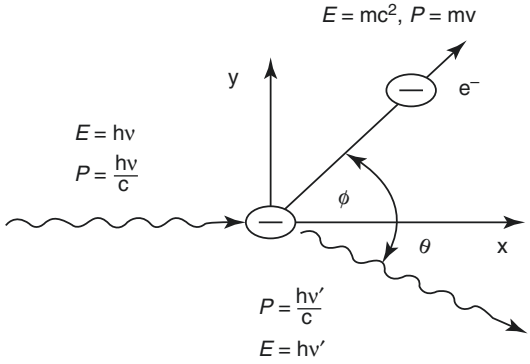

Fig. 1.19 In Compton scattering, incident photon interacts with free electron and deflected by angle θ with energy equal to the difference between incident photon energy and recoil electron

The probability of characteristic x-ray emission decreases as the atomic number of the absorber decreases and thus does not occur frequently for diagnostic energy photon interactions in soft tissue. The probability of this interaction decreases with increasing energy of the incident photon, but increases with increasing atomic number of the absorber.

$$E_e = E_i - E_b \tag{1.19}$$

1.7.2 Compton Effect

Compton scattering is an inelastic collision between gamma ray and valence electron of an atom whose binding energy is much less than gamma ray energy. It is the most prevailing interaction of gamma ray with soft tissue in energy range used for diagnostic purposes. In this mechanism incident gamma photon transfers some of its energy to an electron that assumed to be in rest and known as recoil electron resulting in scattered gamma photon by angle $\underline{\theta}$ with respect to its original path as shown in Fig. 1.19. The energy transferred to the electron is varying depending on the scattered photon angle and can be calculated by applying the laws of conservation of energy and momentum:

$$h\dot{\upsilon} = \frac{h\upsilon}{1+\left(\frac{h\upsilon}{m_e c^2}\right)(1+\cos\theta)} \tag{1.20}$$

where $m_e c^2$ is the rest mass energy of electron (0.511 MeV, refer to Table 1.2). The probability of Compton scattering increases linearly with atomic number of absorber material.

1.7.3 Pair Production

If the gamma ray energy exceeds 1.022 MeV (rest mass energy for two electrons) and passes near to the nucleus, pair production interaction will take place. Conversion of gamma ray energy into two particles (electron and anti-electron) each with mass $m_e c^2$ but opposite electrostatic charge and the total kinetic energy is approximately equal to $hv–2m_e c^2$; therefore, all energy in excess that required to create the pair will be shared by the positron-electron pair as a kinetic energy. After production of a pair, the positron and electron lose their kinetic energy by excitation, ionization and bremsstrahlung as any high-energy electron. When the positron expended all of its kinetic energy, it recombines with an electron, and annihilation phenomenon takes place with production of two photon quanta each of 0.511 MeV released at angle of $180° \pm 0.25°$ relative to each other.

1.7.4 Linear and Mass Attenuation Coefficient

Linear attenuation coefficient (μ_l) is a constant that determines the fraction of radiation beam loss per unit thickness of the absorber because of beam absorption or scatter; in other words, it is a measure of the probability of interaction of photons with matter per unit length. It can be expressed by the following formula:

$$\text{Linear attenuation coefficient } (\mu_l) = \frac{\%\,\text{Reduction in intensity}}{\text{Absorber thickness (cm)}}\,\text{cm}^{-1}$$

Linear attenuation coefficient is specific for each absorber material, but any change in absorber density will change linear attenuation coefficient value. Using mass attenuation coefficient eliminates density dependence of linear attenuation coefficient. Mass attenuation coefficient (μ_m) is given by

$$\mu_m = \frac{\mu_l}{\rho}\ \text{cm}^2/\text{gm} \tag{1.21}$$

where ρ is absorber density in gm/cm^3 and μ linear attenuation coefficient in cm^{-1}

The total linear attenuation coefficients μ is defined as the sum of photoelectric, Compton and pair production attenuation coefficients:

$$\mu = \tau + \sigma + k \tag{1.22}$$

where τ, σ and k are linear attenuation coefficients of photoelectric, Compton interaction and pair production, respectively.

For 511 keV photons produced by positron annihilation, the primary mechanism for photon interaction with matter (one or both annihilation photons) is by Compton interaction while photoelectric absorption is being negligible. From energy dependence point of view, the probability of photoelectric interactions is inversely proportional with cubic photon energy ($1/E^3$); as a result, extreme drop in the probability of photoelectric interaction occurs in a certain absorber material as energy increases, while in Compton interaction, the energy of incident photon must be greater than the electron's binding energy. Therefore, photoelectric interaction is the most preferable interaction for low-energy photons, but as the incident photon energy increases, Compton interaction becomes the most predominant one (Fig. 1.20).

Also, the probability of photoelectric interactions is directly proportional with cubic atomic number of the material (Z^3); thus, the photoelectric interaction is predominant for high Z material. On the other hand, Compton interaction probability depends on electron density (number of electrons/g), and therefore the probability of Compton scattering per unit mass is almost independent of atomic number, and the probability of Compton scattering per unit volume is approximately proportional to the density of the material. In comparison to other elements, the absence of neutrons in the hydrogen atom results in an approximate doubling of electron density. Thus, hydrogenous materials have a higher

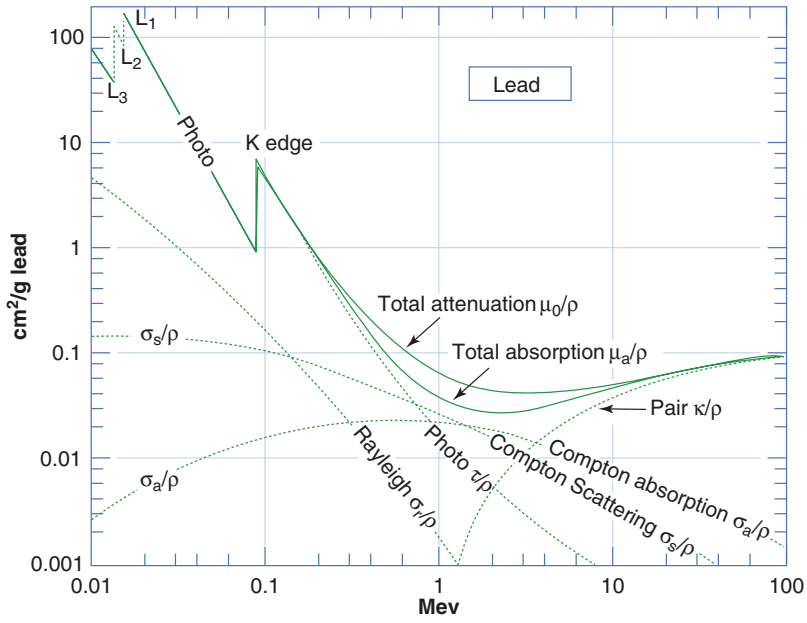

Fig. 1.20 The mass attenuation coefficient of lead (atomic number 82) for gamma rays, plotted versus gamma energy and the contributions by the three interaction effects. Photoelectric effect dominates at low energy. Above 5 MeV, pair production starts to dominate. Compton scattering is the most common interaction at intermediate energies

probability of Compton scattering than a non-hydrogenous material of equal mass.

The product of this form of interaction is that primary photon changes the direction (secondary scattered photon) and loses part of its energy. In addition, the atom where the interaction occurred is ionized. However, when a photon passes through a thickness of absorber material, the probability that it will experience an interaction (removal of photons) is a function of photon energy together with composition and thickness of the absorber. Under conditions of narrow-beam geometry, the transmission of a monoenergetic photon beam through an absorber is described by an exponential function:

$$I(x) = I(0)e^{-\mu_l x} \tag{1.23}$$

where $I(0)$ is the intensity of the un-attenuated photon beam and $I(x)$ is the intensity of photon beam measured at a thickness x through an absorber of linear attenuation coefficient μ_l. The total linear attenuation coefficient of 511 keV gamma rays in tissue is 0.096 cm^{-1}; this corresponds to 7 cm half value layer (HVL = ln2/μ_l). In PET instrumentation, the two annihilation photons interact before escaping the object that is being imaged. The result is that the primary photons are being removed or attenuated from the line of response (LOR) and a potential detection of scattered photons in a different LOR.

1.8 Positron Emitter Radionuclides

As explained above, radionuclides undergoing (β^+) decay are called positron emitters. They differ in the energy of emitted positrons and thus differ in the positron range inside the tissues (the range that the positron travels in tissue depends on the emission energy and the electron density of the surrounding tissue). These radionuclides are used to label a wide variety of pharmaceutical compounds that interrogate disease biochemistry using PET imaging techniques. Briefly, the pharmaceutical interacts with the body through a metabolic process; the radionuclide allows that interaction to be followed, mapped and measured (two annihilation

Table 1.3 The commonly used positron emitters in PET imaging and their physical properties

Radionuclide	Half-life	E_β *max* MeV	$\overline{E_\beta}$ MeV	Percentage of β^+ decays (%)	β^+ max range (mm)	β^+ mean range (mm)	Production method
C-11	20.4 min	0.96	0.39	99	4.1	1.1	Cyclotron
N-13	9.96 min	1.19	0.49	100	5.1	1.5	Cyclotron
O-15	123 s	1.72	0.73	100	7.3	2.5	Cyclotron
F-18	110 min	0.635	0.24	97	2.4	0.6	Cyclotron
Ga-68	68.3 min	1.9	0.84	88	8.2	2.9	Generator (from Ge-68)
Rb-82	78 s	3.35	1.52	95	14.1	5.9	Generator (from Sr-82)

Source: Refs. [2, 6]

photons detected in coincidence). Table 1.3 lists some clinically useful positron emitter radionuclides.

Higher positron energy means a longer effective positron range (the average distance from the emitting nucleus to the end of the positron range) travelling through tissue. For example, in water ^{18}F has low-energy positrons (0.635 MeV) with a very short range (2.4 mm) compared to ^{82}Rb which has high-energy positrons (3.4 MeV) and a longer range (14.1 mm). However, the half-life of radionuclides plays an important role in the availability of the clinical application. Carbon-11, nitrogen-13 and oxygen-15 with very short half-lives can only be used to study processes that have rapid uptake. Fluorine-18 with an approximately 2 h half-life allows more time for synthesis, tracer uptake and for imaging particularly in diagnostic applications of oncology.

1.8.1 Exposure Rate Constant

Before discussing the emission rate and exposure levels of positron emitter radionuclides, it would be appropriate to understand some basic definitions in this context. In terms of energy levels, one can note that radiation of energy >20 keV (lower energy does not contribute to radiation exposure) interacts with an absorbing medium (air or patient) to deposit energy producing positive and negative ions or what is called ionization. The amount of ionization of air caused by a γ-ray or x-ray source is defined as exposure, whereas the sum of the kinetic energy of all charged particles produced by interactions from a source of x-rays or γ-rays (through Compton scatter, photoelectric absorption or pair production) per kg of air is known as air kerma. The relationship between exposure, *X*, and air kerma, *K*, can be calculated as:

$$K\left(\mathrm{Gy}\right) = X\left(R\right) \times 0.00869$$

The radiation exposure level from gamma and x-ray sources can be estimated from the exposure rate constant Γ which is defined as the exposure rate in μSv/h from 1 mCi (37 MBq) of a radionuclide at a distance of 1 m. Each radionuclide has a specific value of exposure rate constant (Table 1.4). Precisely, while calculating the exposure rate constant of radionuclide, all emitted radiations from that source must be considered, and adjustments should be made for any attenuating medium (air or patient) between the source and the point of interest. Therefore, each radionu-

Table 1.4 Summary of exposure rate constant for different radionuclides used in nuclear medicine procedures

		Dose rate constant μSv.m^2/MBq.h	
Nuclide	Half-life (h)	Point source	Patient
Ga-67	78.1 h	0.028	0.011
Tc-99m	6.02 h	0.0195	0.0075
In-111	2.8 days	0.086	0.03
I-123	13 h	0.041	0.015
I-131	8.06 days	0.0575	0.023
Xe-133	5.3 days	0.135	0.006
F-18	110 min	0.143	0.092

Source: Refs. [10, 13]

clide represents an exposure rate constant for a point source geometry different than being in vivo (patient body). Due to body attenuation (the body absorbs some of the annihilation radiation), the dose rate from the patient is reduced by a significant factor (self-absorption). For example, the exposure rate of ^{18}F as a point source is 0.143 μSv.m^2/MBq.h, whereas the patient exposure rate is significantly lower (0.092 μSv.m^2/MBq.h) accounting for 36 % photon reduction.

The exposure rate in air at a given distance:

$$\Gamma = \frac{1}{4\pi}\sum_i \left(\mu_{en}/\rho\right)_i Y_i E_i \qquad (1.24)$$

where (μ_{en}/ρ) is the mass-energy absorption coefficient in air for photons of energy E_i emitted by the nuclide with yield Y_i. To estimate the exposure rate (dose rate) from a source of (mCi) activity at a certain distance (m), the following relation may be used:

$$D\left(\mu Sv/h\right) = \frac{\Gamma A}{d^2} \qquad (1.25)$$

where Γ is the exposure rate constant also known as gamma constant (μSv m^2/MBq h), A is the activity (MBq) and d is the distance (m). In radiation shielding, it is therefore of economic value to use the most appropriate exposure rate constant provided the different conditions including the type of radionuclide, exposure rate constant, uptake time, imaging time, occupancy factors and other variables that may exist in PET or SPECT imaging environments. See Chap. 2 for further details on facility design and other shielding calculations.

1.9 Radiation Detection and Measurements

Radiation detection and measurements are cornerstone activities in nuclear medicine daily practice. It includes many of the hot laboratory equipments, radio-pharmacy, radiation safety and protection, assay counting as well as scanning examinations. All of these require similar or different concepts of radiation detection and/or measurements. We will discuss here the most important radiation equipments involved in dose measurements and counting taking the most typical examples which are dose calibrator and well counter. Other detection devices such as gas-filled detectors, scintillator as well as semiconductor-based detection systems will also be outlined.

1.9.1 Gas-Filled Detector

Gas-filled detectors consist of a chamber filled with a volume of pressurized gas usually at a pressure of one atmosphere or less, to enhance interactions of radiation as it passes through the medium. Radiation that passes through the medium results in gas molecule ionization, followed by collection of the ion pairs with the application of a voltage between the two electrodes. Ions produced are collected as current and amplified to record the resultant signal. The collection of the ion pairs is a function of the applied voltage, radiation energy, intensity levels and type of the gas.

At very low voltage (<10 V), not all the ion pairs could drift towards the electrodes and be collected; some ion pairs recombine to form the original molecule (not enough acceleration). This region is called the region of *recombination*. As voltage increases (>10 V), recombination becomes negligible, and the entire ion pairs can be collected efficiently by the electrodes. The applied voltage changes do not affect the produced current, current remains the same as it called the saturation current, and it is proportional to the deposit ionization energy of the incoming radiation (alpha, beta, gamma). Hence, the region is called the *ionization region* (50–300 V).

Raising the applied voltage to a higher value provides the ion pairs (primary ionization) with a higher energy and velocities and enables them to collide with the medium forming a secondary ionization. Hence, increasing the voltage that provides each electron with the enough energy to produce a secondary ionization, a multiplication of charges and amplification of the produced ionization is proportional to the initial ionization. This region is called the *proportional region*. Beyond that voltage range, the proportionality

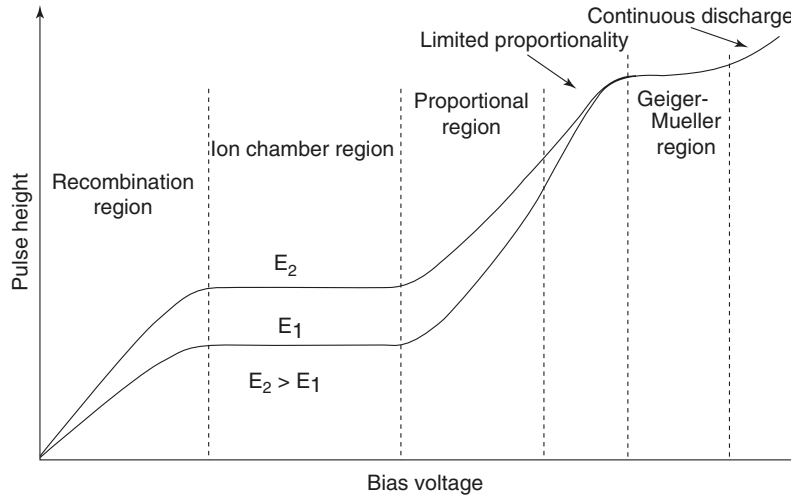

Fig. 1.21 Types of operational voltage regions of gas-filled detector as a result of two different energies of incident photons

becomes limited as the multiplication of charges increases rapidly (limited *proportionality* region). Further increased voltage, the yielded current is of identical behaviour for all types of radiations forming a plateau as voltage increases. This region is referred to *Geiger-Mueller* region. At very high voltage, *continuous discharge* region begins in which a spontaneous ionization is taking place inside the chamber; using a detector at such high voltage might destroy it. Figure 1.21 is showing the various operating voltage regions.

Different types of radiation lead to different ion pair production, since the interaction of the ionizing particle/photons with gas molecules is different. Alpha, beta and gamma radiation could be detected using the gas-filled detector types (i.e. ionization chamber, proportional counter and Geiger-Mueller counter).

An important application of ionization chamber principle is for CT dosimetry measurement purposes through the usage of CT ionization pencil chamber. The ionization pencil chamber is used for the evaluation of computed tomography dose index (CTDI) either in air or mounted in acrylic or polymethyl methacrylate (PMMA) phantoms (head, 16 cm, and body, 32 cm in diameter for adult). It is a pencil-shaped chamber with about 10 cm sensitive length specifically designed for x-ray beam measurements and can be connected to electrometer. It has an excellent energy and partial volume response along its entire length. Hence, it produces an accurate dose estimate by irradiating its entire volume. It also provides uniform response to incident radiations in every angle around its axis and therefore can fit the dosimetric conditions required for dose estimate in CT imaging procedures. Figure 1.22 is showing an ionization chamber and PMMA phantoms used in CT dosimetry. Further details on CT dosimetry can be found in Chap. 2.

1.9.1.1 Dose Calibrator

Dose calibrator contains an argon gas-filled ionization chamber coupled to a high voltage power supply and an electronic circuit that converts and displays chamber response in units of activity. The ionization chamber is under high pressure (increases detection sensitivity), sealed (eliminates the need for temperature and pressure correction) and contains two electrodes having an electric potential between them. A beam of ionizing radiation passes through the chamber and produces electrical charges that are collected by positive (anode) and negative (cathode) electrodes forming total amount of current (time-averaged ionization current). This amount of current is measured by using sensitive current-measuring devices called electrometers (quantify very small electric currents of fA to μA, corresponding to

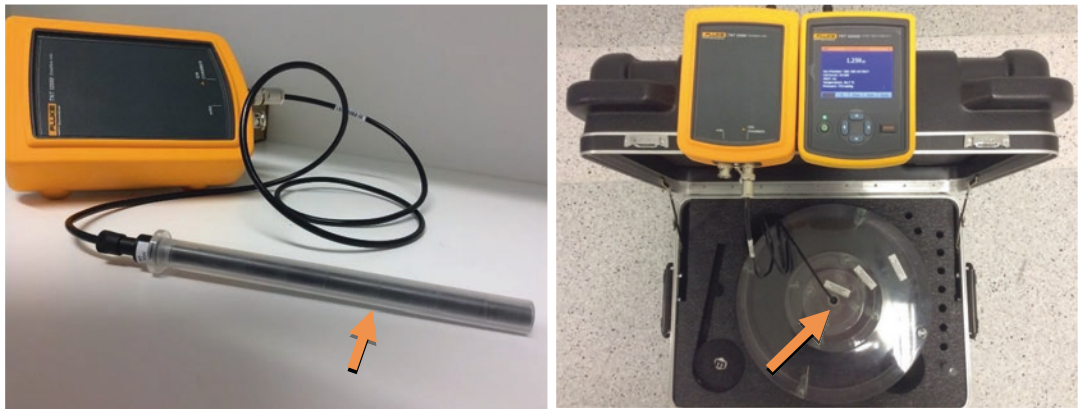

Fig. 1.22 Photographs showing one of the commercially available ionization chamber that is in operation in our laboratory (Courtesy of Fluke Biomedical). *Arrows* indicate ionization chamber (*left*) inserted into one of the phantom wells used in CT calibration (*right*)

10^{-15} and 10^{-6} Ampere, respectively). The current generated in the circuit is proportional to the activity of the measured quantity. Shielding is used around the chamber to reduce the effect of background radiation and to reduce unnecessary operator exposure.

A dose calibrator is used for assaying activities of radiopharmaceutical (γ-rays emitters) of relatively large quantities (i.e. MBq range) placed in vials and syringes. It is calibrated to read directly in units of activity (becquerels or curies) with the ability of choosing the radionuclide type and volume (specifying calibration factor). Dose calibrator's chamber response depends on the specified radionuclide source geometry, its type of decay, energy of emission and source position inserted. For example, the chamber response to pure gamma emitter radionuclide (^{99m}Tc) is different than for a combination of beta and gamma emission (e.g.^{131}I). However, calibration factors assure the accurate activity reading for a selected radionuclide source in the specific geometry being used.

Despite the high range of activity that the dose calibrator can measure, it is relatively insensitive and cannot accurately assay activities less than 1 μCi. Furthermore, the ionization chamber has no ability to distinguish photons of different energies as is possible with detectors having pulse-height analysis capabilities. However, dose calibrators are of great importance in nuclear medicine departments to check every radiopharmaceutical dose that is received or dispensed. Also, they are used to assay the activity of various types of radiopharmaceuticals prior to clinical usage. Therefore, dose calibrator's operation must be checked in a daily basis to assure the desired continued accuracy of the dosage assays (≤5 % accuracy), and several quality control tests need to be performed and repeated at specific intervals (see Table 1.5).

1.9.2 Well Counter

Well counter is a highly efficient radiation detector for counting low-level radioactive samples such as blood or urine collected from radioactive patients, wipes of contamination and any source of activity in the range of micro-curies. Well counters consist of a single solid cylindrical crystal of thallium-doped sodium iodide-NaI(Tl) detector with a hole in the centre for a sample to be placed. It is coupled to photomultiplier tube (PMT) and its associated electronics such as preamplifier, amplifier, pulse-height analyzer (PHA) and scalar-timer. Dimensions of such NaI(Tl) crystal detectors are in the range of:

- 4.5–12.7 cm diameter
- 5–12.7 cm long

Table 1.5 Recommended quality control programmes for a local dose calibrator

Test type	Frequency	Acceptance criteria
High voltage	Daily	Comparable with the manufacture's tolerances
Zero adjustment	Daily	Comparable with the manufacture's tolerances
Background	Daily	Within normal range comparable with the environmental facility
Constancy (check source)	Daily, annually	Within ±5 % of the decay corrected initial value
Accuracy	Annually	Within ±5 % of the decay corrected initial value
Reproducibility (precision)	Annually	Within ±1 % of the average measurements
System linearity	Annually	Within ±5 % of the expected values
	Quarterly	Within ±2 %
Supplier equivalence	Annually	Differences ≤ ±10
	Acceptance (initially established)	Differences ≤ ±5

Table taken from Ref. [9]
Daily means every 24 h starting at 12:00 a.m.

And the well dimension can have the following measures:

- 1.6–3.8 cm diameter
- 3.8–7 cm depth length

A thickness of 5 cm or greater of lead is commonly placed around the detector to reduce background counting levels. Small well counters are used for low-energy gamma rays detection (<200 keV), whereas larger well counters are used for high-energy gamma rays.

Since the inserted sample in the well counter is surrounded by the scintillation crystal, NaI(Tl) detectors have high intrinsic and geometric detection efficiencies of gamma rays; only small amounts of activity can be counted up to about 1 μCi (37 kBq). At higher activities, serious dead time problems do emerge leading to count rate underestimation. The detection efficiency of well counter device is a function of photon energy and detector thickness. For example, the detection efficiencies of a commercially available well counter installed in our laboratory for the radionuclides ^{99m}T, ^{131}I and ^{18}F are 81.66 %, 28.70 % and 28.25 %, respectively.

1.9.3 Scintillation Detectors

Although scintillation mechanism is one of the oldest technical methods for detection of ionizing radiation, it is still widely used as a radiation detector. As outlined above, there are a number of available technologies that can be used in photon detection with relative advantages and technical merits. Scintillator detectors can be used with cost-effective and feasible manner to be incorporated in many imaging systems. It has been used in the manufacturing of SPECT systems, survey metres for energy discrimination and high-efficient radiation detectors as well as in PET imaging scanner including clinical and preclinical systems. Scintillation detectors can be classified into:

I. Inorganic scintillation detectors, e.g. alkali halide scintillator (NaI, CsI, etc.) in the form of solid crystal
II. Organic scintillators which can be pure organic crystal, liquid organic solutions or polymers known as plastic scintillators

The basic difference between organic and inorganic scintillator is the light production mechanism. In case of inorganic scintillator, the light emitted by an inorganic crystal is primarily

due to the crystal structure, whereas organic substances exhibit luminescence by virtue of molecular properties.

The ideal scintillation material should possess the following properties:

1. *High stopping efficiency*. Scintillator material should have high efficiency for converting incident radiation energy into emitted luminescence. Scintillator with high effective Z and high density is a better candidate as the former is proper for photoelectric interaction, while the later serves to dominate Compton interaction.
2. *High-energy resolution*. This feature plays an important role in removing scattered radiation. It can be improved by using crystals of high light output and efficient electronic circuitry.
3. *Transparency*. The medium should be transparent to wave length of its own emission for good light conversion and reduction of light loss. The light readout photosensor should also have optical properties that fit the wavelength range of the emitted photon quanta from the scintillator.
4. *Short decay constant*. Short decay constant is a desired property that helps improve coincidence timing resolution as well as an important factor in count rate performance and reduction of dead time. Random coincidences can also be reduced by using crystal of short decay time. Crystals of short decay time are also better candidates in time of flight applications.
5. *High light yield*. The material should be of good optical yield and has a size large enough to use as practical detector. As the crystal dimension decreases in size to improve spatial resolution, as in block detector design of PET scanners, it is necessary to have a scintillator of high light output. As outlined above, light yield also improves timing and energy resolution.

No material can fit all of these properties, and therefore it is usually a trade-off process favouring some properties over the others. For diagnostic purpose, the use of inorganic alkali halide crystal doped with thallium such as NaI(Tl) is widely applied in gamma camera and SPECT imaging systems. In PET imaging, BGO crystal and LSO-type detectors occupy the most important class of scintillator in the market with much interest given to the later due to its better physical properties that fit into state-of-the-art PET clinical applications. Table 1.6 summarizes the physical properties of some crystals used in PET imaging scanners.

The scintillation light is emitted isotropically and optically coupled to the photocathode of a PMT. Scintillation photons incident on the photocathode liberate electrons through the photoelectric effect, which are then accelerated by a strong electric field in the PMT. As these photoelectrons

Table 1.6 Physical properties of some useful inorganic scintillation crystals used in PET

	NaI(TI)	BGO	GSO:Ce	LSO:Ce	LYSO:Ce	$LaBr_3$	BaF_2
Density (gm/cm^3)	3.67	7.13	6.7	7.4	7.1	5.3	4.89
Effective atomic number (Z)	51	74	59	66	64	47	54
Linear attenuation coefficient (cm^{-1})	0.34	0.92	0.62	0.87	0.86	0.47	0.44
Light yield (% NaI[Tl])	100	15	30	75	75	160	5
Decay time (ns)	230	300	60–65	40	41	16	0.8
Hygroscopic	Yes	No	No	No	No	Yes	Slightly
Photoelectric effect (%)	17	40	25	32	33	13	12
Refractive index	1.85	2.15	1.85	1.82	1.81	1.88	1.56
Emission maximum (nm)	410	480	440	420	420	370	220

are accelerated, they collide with electrodes in the tube (known as dynodes) releasing additional electrons. This increased electron flux is then further accelerated to collide with succeeding electrodes, causing a large multiplication (by a factor of 10^5 or more) of the electron flux from its initial value at the photocathode surface. Finally, the amplified charge burst arrives at the output electrode (the anode) of the tube. The magnitude of this charge surge is proportional to the initial amount of charge liberated at the photocathode of the PMT; this is defined as the gain of the PMT.

Furthermore, by virtue of the physics of the photoelectric effect, the initial number of photoelectrons liberated at the photocathode is proportional to the amount of light incident on the PMT which in turn is proportional to the amount of energy deposited in the scintillator by the gamma ray (assuming no light loss from the scintillator volume). Thus, an output signal is produced that is proportional to the energy deposited by the gamma ray in the scintillation medium. However, the spectrum of deposited energies (even for a monoenergetic photon flux) is quite variable because of the occurrence of the photoelectric effect, Compton scattering, various scattering phenomena in the scintillation medium and statistical fluctuations associated with all of these processes.

1.9.4 Neutron Detectors

Neutrons are neutrally charged particles that maintain the nuclear binding stability by moderating the repulsion force exhibited by protons. The story of discovering neutrons by James Chadwich in 1932 and its properties is central to the extraordinary developments in atomic physics that took place in the early decades of the twentieth century. Neutrons are not essential part of daily practice for those who are working in nuclear medicine environment. However, it has some significant concerns in medical cyclotrons and shielding construction as well as in operation of nuclear reactors. The former is our focus, and therefore some information about neutron detectors can be useful to mention here. Neutrons are classified according to their energy into:

1. Thermal neutrons in energy range of 0.025 eV up to 0.2 eV at 20.44 °C
2. Slow neutrons with energy between 1 and 10 eV, sometimes up to 1 keV
3. Fast neutrons which have energy above 0.5 MeV

Due to the well-known fact that neutrons are uncharged particles, it is therefore cannot be detected in a direct way. It can be measured via their interactions with atoms to produce a kind of radiation that can be detected in one of the conventional methods. The most common nuclear reactions for thermal neutrons detection are through (n, α) or (n, p) reactions using ${}_5{}^{10}B$, ^{6}Li and ^{3}He. There are two other methods that depend on (n, fission) reactions and neutron activation. The former is based on fission fragments detection, while the latter utilizes the emissions of the radioactive produced nuclei to detect neutron flux.

Boron-trifluoride proportional counter is used in case of ^{10}B (n, α) reaction which uses BF_3 as proportional gas and neutron detection material. Boron has a high interaction cross section (4010 barns) for this reaction. The BF_3 gas is usually enriched in ^{10}B, and it has to be used at lower absolute pressures in order to get a good performance as a proportional gas.

Similarly, ^{3}He is used as a conversion target and proportional gas in the ^{3}He proportional counter. But ^{3}He(n, p) reaction shows low Q-value of almost 765 keV. As a result the discrimination of gamma rays is more difficult than with BF_3 counters, since secondary electrons only deposit a small amount of energy in the gas.

Instead of using the gas-filled proportional counter, Li has also a good interaction cross section for (n, α) reaction and has been used in a neutron scintillator detector in the form of europium (Eu)-doped lithium iodide crystal. Due to the density of enriched ^{6}LiI(Eu) crystals, a 10 mm-thick detector is almost 100 % efficient for neutrons ranging from thermal energies up to about 0.5 eV.

However, some modification in the neutron detection system should be considered in case of intermediate and fast neutrons such as adding

moderator material to slowing down neutrons to energies where the detection efficiency is high. Materials such as polyethylene and paraffin are the most widely used moderators. The use of moderator in case of fast neutron is no longer effective, and thus fast neutron detection depends on elastic scattering with light nuclei. Therefore, fast neutrons incident on a hydrogen-containing scintillator will scatter elastically and give rise to recoil protons ranging in energy up to the full neutron energy. Fluorescence light is emitted as the recoil protons energy is absorbed by the scintillator. A series of spheres of different diameters were developed to thermalize neutrons of low, medium and higher energies. This method allows one to detect neutron energy flux of different energies or neutron energy spectrum.

1.9.5 Solid State Detectors

A semiconductor detector acts as a solid-state ionization chamber. Ionization will take place in the sensitive volume of the detector as ionized particle hit the detector. The charge produced by the photon interactions is then collected directly. The operation of semiconductor detector depends on having either excess electrons or holes which depend on the impurities added to pure semiconductor material. The sensitive volume in the detector is an electronically conditioned region (known as the depleted region) in which liberated electrons and holes move freely.

Germanium (Ge) and silicon (Si) are the most common semiconductor used to construct solid-state detectors. The detector functions as a solid-state proportional counter, with the ionization charge swept directly to the electrodes by the high electric field produced by the bias voltage. The early design of solid-state detector used lithium-drifted germanium [Ge(Li)] as the detection medium. The lithium served to inhibit trapping of charge at impurity sites in the crystal lattice during the charge collection process. Hyperpure germanium (HPGe) crystals were then used with no further doping, and detector operation became more simple. Cooling is one drawback of HPGe detector but serves to reduce thermal excitations of valence electrons. This makes the incident gamma radiation provide the energy necessary for the electrons to cross the band gap and reach the conduction band.

Recently, cadmium telluride (CdTe) and cadmium zinc telluride (CdZnTe or CZT) started to be used as solid-state detector in SPECT modalities as well as in prototype PET scanners. The former has density of 6.06 g/cm^3 and atomic number Z of 48. CZT is CdTe in which some of the Te atoms (typically 20 %) are replaced by zinc atoms. Average energy expended per electron-hole pair created is 4.4 eV, while the ionization energy for dry air is 34 eV. These measures make this type of detectors amenable

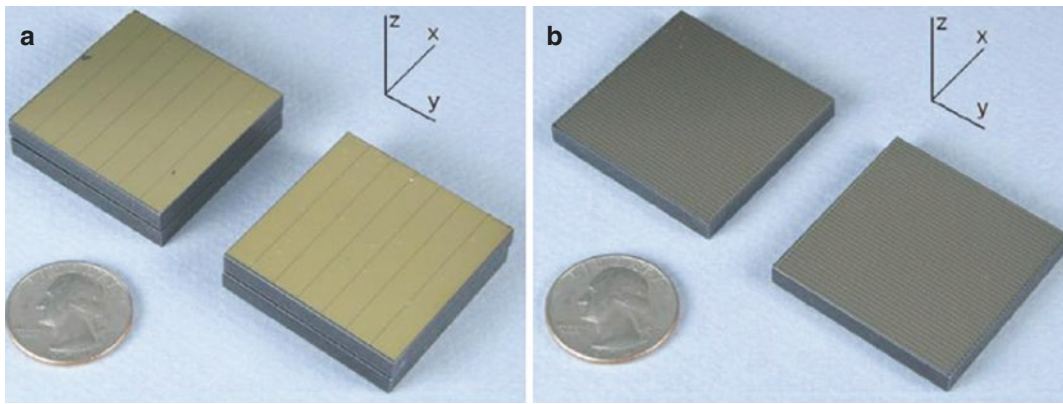

Fig. 1.23 Cross-strip of CZT detector with dimensions 4 × 4 mm × 0.5 mm, cathode (**a**) and anode (**b**) (Reprinted from Gu et al. [20] with permission)

for good stopping efficiency against gamma radiations. In addition, it is featured by room temperature operation without excessive electronic noise. Due to some manufacturing limitations and cost-related issues, the use of CdTe and CZT is confined to small-sized counters or imaging systems, such as micro-PET imaging systems.

In small animal PET, the aim of CZT scanners is to improve system spatial resolution achieving almost 1 mm with recent submillimetre resolution in experimental setup using very small pitch pixelated detector. In general, the spatial resolution of a pixelated CZT detector is limited by the anode pixel size. In addition, the spatial resolution is also affected by the charge sharing between the neighbouring anode pixels that collect the electrons created after gamma ray interactions. Also, one of the major challenges in using pixelated CZT detectors is to read out the large number of channels of anode signals with high accuracy and efficiency.

CZT-based PET detector with 4 cm thickness introduces intrinsic detection efficiency exceeding 86 % for single 511 keV photons (>73 % for coincidence photons). Furthermore, CZT detector has superior energy resolution better than 3 % full width at half maximum at 511 keV. This feature allows one to design a system with significant reduction of scattered radiation, random events and better accuracy of event localization. However, the major drawback of CZT detector as PET detector is the poor timing performance due to variability in charge movement. Figure 1.23 shows cross-strip CZT detector.

References and Further Reading

1. Evans RD. The atomic nucleus. McGraw-Hill, New York; 1955.
2. Cherry SR, Sorenson JA, Phelps ME, editors. Physics in nuclear medicine. 4th ed. Philadelphia: W.B. Saunders; 2012.
3. Martin James E. Physics for radiation protection. 2nd ed. Weinheim: Wiley-VCH Verlag GmbH & Co. KGaA; 2006.
4. Khalil MM, editor. Basic sciences of nuclear medicine. Heidelberg/Dordrecht/London/New York: Springer; 2011.
5. Ahmed Syed N. Physics and engineering of radiation detection. Britain: Elsevier; 2007. ISBN 13: 978-0-12-045581-2.
6. Freeman LM, Biersack H-J, editors. Clinical nuclear medicine. Germany: Springer; 2007. 24/3150-543210.
7. Sharp PF, Gemmell HG, Murray AD, editors. Practical Nuclear Medicine. 3rd ed. Oxford University/Verlag/London: Springer; 2005.
8. IAEA human health reports No.5. Status of computed tomography dosimetry for wide cone beam scanners. 2011.
9. AAPM REPORT NO. 181; The selection, use, calibration, and quality assurance of radionuclide calibrators used in nuclear medicine. Report of AAPM Task Group 181. 2012.
10. Madsen MT, Anderson JA, Halama JR, Kleck J, et al. AAPM Task Group 108: PET and PET/CT shielding requirements. Med Phys. 2006;33(1):4–15.
11. Mohr PJ, Taylor BN, Newell DB. CODATA recommended values of the fundamental physical constants: 2010. NIST.2012. p. 1–94.
12. Pillai MR, Dash A, Knapp Jr FF. Sustained availability of 99mTc: possible paths forward. J Nucl Med. 2013;54:313–23.
13. IPSM. Radiation protection in nuclear medicine and pathology. In: KE Goldstone, PC Jackson, MJ Myers, AE Simpson, editors. Report No 63, York: Institute of Physical Sciences in Medicine; 1991.
14. Saha GB. Fundamentals of nuclear pharmacy. 6th ed. New York/Heidelberg/Dordrecht/London: Springer; 2010.
15. Shankar V, editor. Molecular imaging: radiopharmaceuticals for PET and SPECT. Dordrecht/Heidelberg London/New York: Springer; 2009. ISBN 978-3-540-76734-3.
16. Basdevant JL, Rich J, Michel S. Fundamentals in nuclear physics. New York: Springer Science + Business Media, Inc.; 2004.
17. Sarah K, editor. Passive nondestructive assay of nuclear materials. Nuclear Regulatory Commission, Washington U.S., Springfield; 1991.
18. Dewan L. Design and construction of a cyclotron capable to accelerating protons to 2 MeV. Massachusetts Institute of Technology, Department of Nuclear Science and Engineering; 2007.
19. Friesel DL, Antaya TA. Medical cyclotrons. Cambridge: Massachusetts Institute of Technology; 2007.
20. Gu Y, Matteson JL, Skelton RT, Deal AC, Stephan EA, et al. Study of a high-resolution, 3D positioning cadmium zinc telluride detector for PET. Phys Med Biol. 2011;56:1563–84.
21. Baumann T. Minicourse on experimental techniques at the NSCL neutron detection & spectroscopy. National Superconducting Cyclotron Laboratory. Michigan State University, East Lansing, Michigan; 2001.
22. Smith DS, Stabin MG. Exposure rate constants and lead shielding values for over 1,100 radionuclides. Health Phys. 2012;102(3):271–91.
23. Podgorsak EB. Radiation physics for medical physicists. Germany: Springer; 2006.